The variation of the relative intensity of cavitation with temperature

M. I. Ibisi

THE VARIATION OF THE RELATIVE INTENSITY OF CAVITATION WITH TEMPERATURE.

By

M.I. IBISI, B.Sc., Grad.Inst.Phy.

Presented in candidature for the degree of Master of Science of the University of Durham.

Michaelmas 1966.

ILLUSTRATIONS.

Fig. No.

3.1 Relative deformation ($\Delta L/L$) as a function of field strength for nickel and cobalt. (From figure in "High Intensity Ultrasonics" by Brown and Goodman[1.4], page 76).

3.2 Shapes of magnetostrictive transducers: 1. the simple rod, 2. the tube, 3. the laminated rod, 4. Laminated rod with slot, 5. Laminated window type, 6. Laminated ring, (cut away). 7. Laminated cylinder. (From "Ultrasonics" by Carlin [1.3] page 108).

3.3 The Equivalent circuit of a magnetostrictive transducer. (From "Ultrasonics" by Vigoureux [1.2] page 24).

3.4 A typical oscillator for driving magnetostrictive transducer unit. (Personal circuit diagram based on advice by Grange [2.25]).

The following :-

3.5 Block diagram of the electronic generator.

3.6a Front view of the 2.0 KW generator for driving magnetostrictive transducer unit.

3.6 b Rear view of the 2.0 KW generator for driving magnetostrictive transducer unit.

3.7 Circuit diagram of the 2.0 KW generator. The chassis are numbered from top to bottom

are diagrams of a specially modified version of the Rapiclean unit manufactured by Ultrasonics Ltd.

3.8 Operational characteristics of the 2.0 KW generator for four values of magnetization current. (The points used are my personal results obtained during the preliminary experiment.)

3.9 Flang mounted probe surrounded by metal cage and cooled by air blower.

3.10 Typical magnetostrictive transducer unit coupling system.

(3.9 and 3.10 are diagrams of laboratory equipments used for demonstration).

Fig. No.

3.11 Suspension Device used in cavitation activity measurements. (Designed and constructed by the candidate).

3.12 Experimental set-up. A.Constant temperature tank, (part of the complete set of equipments supplied by Ultrasonics Ltd.) B. Suspension Device, C.Test tube, D. Mercury-in-glass thermometer. The generator is at the background.

4.1 Cavitation erosion as a function of temperature for aluminium in water. (From figure in "High Intensity Ultrasonics" by Brown and Goodman [1.4], page 48).

The following :-

4.2 A typical absorption spectrum for yellow solution.

4.3 Absorption spectrum with broad peak indicating an excess of chlorine radical.

4.4 Evaporation test. (a) Absorption spectrum for first test solution. (b) Absorption spectrum for second test solution, warmed to 50°C and cooled to 20°C before irradiation.

4.5 Erosion pattern on a lead sample after 40 minutes exposure to cavitation. "A" is the metal wire threaded through the hole, B.

are results obtained by the candidate.

5.1 Optical density as a function of temperature for a mixutre of CCl_4 solution and O-tolidine reagent. (Graphical representation of Eqn. 5.2 and results of Table 5.1)

5.2 Cavitation erosion as a function of temperature for lead in water. (Graphical representation of Eqn. 5.3 and results of Table 5.2).

P.S. Figures from "Cavitation Damage" by Eisenberg [2.27] are set at the end of the Report and the pages are not numbered.

ABSTRACT.

The variation of the relative intensity of cavitation with temperature has been determined by the chlorine liberation and erosion methods. Cavitation ability determined by the erosion method has been studied over a temperature range of 20° to 80°C and for an ultrasonic irradiation period of 40.0 ± 0.04 minutes, using lead plates as samples. Studies of the free radical formation ability of cavitation over the same temperature range and for an irradiation time of 120.0 ± 0.1 seconds are described.

Factors such as the standardization of solutions, evaporation of solution, the preparation of lead samples and their effects on the experimental results are accounted for. The endeavour has been to conduct these experimental assessments of cavitation ability under identical conditions of transducer frequency, power input to the transducer, height of test samples over the transducer face, etc., and to obtain mathematical expressions in respect of the two activities of cavitation.

A comparison of the results with previous experimental observations and their suitability as industrial methods of assessing ultrasonic cleaning effectiveness have been discussed. The possibility of measuring the relative intensity of cavitation and determining industrial ultrasonic cleaning efficiency with a piezoelectric crystalline probe is suggested.

An electronic generator with a variable power out-put of 2 kw, capable of driving a magnetostrictive transducer unit at a frequency of 20 kc/s and used in the experimental work is also described.

ACKNOWLEDGEMENTS.

The work described in this thesis was carried out in the laboratories of the Royal College of Advanced Technology, Salford, between November 1964 and February 1966. The author would like to offer his sincere thanks to Dr. B. Brown and Dr. J.A. Apostolakis for their patient supervision of the work and for their time given to many helpful discussions.

The author also wishes to express his gratitude to Mr. K. Eng for his interest and advice in the preparation of lead samples, to Dr. M.A. Slifkin for the use of his spectrophotometer, to Mrs. W. James for her help in the writing of the computer programme, and to the Governors of the College for the provision of a research grant.

CONTENTS.

CONTENTS (Continued)

CHAPTER 1.

WAVE PROPAGATION.

The term "wave motion" denotes a condition that is somehow transmitted so that it can be experienced at a distance from where it was originally generated. It involves the generation of vibrations of the body which provides the source of energy and of the elementary particles in the medium through which the waves are passing. Sound waves are a form of wave motion the transmission of which is supported by all materials that possess elasticity. Elasticity provides a restoring force on the particle while inertia causes the particle to oscillate about a mean position. Where the particles of the medium vibrate in the direction of wave motion, they give rise to alternate compressions and rarefactions in the medium, and they are termed longitudinal or L waves. When the direction of motion of the particles is normal to the direction of propagation of waves, they give rise to alternating shear stresses in a bulk medium and they are termed shear or transverse waves.

Where the source of energy is a periodic force, $F = F_o \text{ Sin } wt$, of frequency, $f = {}^{w}/_{2\pi}$, the particle experiences forced oscillations and also some damping due to frictional forces. The frequency of oscillation of the mass is the same as that of the force; and for small damping, the frictional force is proportional to the velocity of the particle. The equation of motion is [1.1]

$$M \frac{d^2x}{dt^2} + R \frac{dx}{dt} + \frac{x}{C_m} = F_o \text{ Sin } wt \qquad 1.1$$

where x is the displacement of the particle at any time, t; M is the mass of the particle, R is the mechanical resistance and C_m is the displacement per unit restoring force.

Under steady conditions, the velocity, U, is given by

$$U = \frac{F}{R + j(wM - {}^{1}/_{wC_m})} \qquad 1.2$$

where $j = (-1)^{\frac{1}{2}}$; and the velocity amplitude is

$$U_o = \frac{F_o}{R^2 + (wM - {}^{1}/_{wC_m})^2}^{\frac{1}{2}} \qquad 1.3$$

In comparison with an electrical circuit containing a resistance, R, an inductance, L, and a capacitance, C, in series with an alternating e.m.f., V; R, M, C_m, and F in equations 1.1, 1.2, 1.3 are analogues to R, L, C, and V respectively. x and U are equivalent to the electrical charge, q, and, current, i, respectively. When $f = {}^{w_r}/_{2\pi} = {}^{1}/_{(MC_m)^{\frac{1}{2}}}$; the velocity amplitude is a maximum, the reactive component $X = (wM - {}^{1}/_{wC_m})$, of the mechanical impedance, $(Z_m = {}^{F}/_{u})$, is zero; and resonance is said to occur. The quality of resonance is described by the mechanical "Q" factor (Qm); and is given by

$$Qm = \frac{w_r M}{R} \qquad 1.4$$

where w_r is the resonance angular velocity.

1.2 ULTRASONICS.

DEFINITION AND TYPES OF WAVES:

Vibratory waves of a frequency above that of the upper frequency limit of the human ear are referred to as ultrasonics. It embraces all frequencies above about 16 kc/s, although the term is also loosely applied to frequencies in the sonic range used for certain ultrasonic applications. The upper frequency range in the neighbourhood of about 500 Mc/s is imposed by practical limitations.

Ultrasonic waves are a special form of acoustic waves and like sound waves, they depend essentially on particle vibration for their transmission through a medium. The equations given above apply to ultrasonic waves provided they are propagated in a medium that satisfies the conditions governing the derivation of the equations.

In practice, several conditions both in the method of generation of waves and in the medium supporting ultrasonic waves lead to rigorous modifications of the equations of Section 1.1. Like all acoustic waves, ultrasonic waves can be propagated as longitudinal (L - waves) or transverse (S - waves), waves. Generally, the medium into which the wave is propagated and the method of applying the propagating source to the medium, decide the pattern of the vibratory path taken by successive elements of the medium. Waves can also be propagated over a surface without influencing the bulk of the medium below the surface. These are known as Rayleigh waves.

ULTRASONIC PROPAGATION THROUGH MEDIA:

Not all media support all types of waves. Liquids and gases generally do not support S-waves but solids can support all forms of waves. Volume changes in the medium sometimes occur due to the passage of waves; and this leads to a second method of the classification of waves. Experimentally, longitudinal waves are almost entirely dilatational waves as they produce volume changes in the medium, while shear waves do not produce these changes and are classes as distortional waves. Longitudinal waves have a high velocity of travel in most media and are most often used in ultrasonic applications since they can be propagated in both solids, liquids and gases. Shear waves have a lower velocity - about one-half of that of the L waves; and because of this, the wave-length of S waves is much shorter than that of L waves. Because of the latter, S waves are more sensitive to inclusion in a medium and they are therefore more easily scattered within a material.

The passage of ultrasonic waves through a medium generally results in energy dissipation due to scattering, viscosity or damping effects, and to heat conduction and radiation between the rarefaction and compression sections of the wave. If the energy density is E, then, the intensity I in a non-absorbing medium is

$$I = cE$$

where c is the velocity of the wave in the medium. In an absorbing medium,

$$I = I_o \exp(-2\alpha x) \qquad 1.5$$

where $I = I_o$ for $x = 0$ is the boundary condition; and α is the co-efficient of absorption of the medium.

Absorption of energy due to thermal effects is commonly observed at megacycle frequencies. The flow of energy is from regions under compression and at higher temperatures, to those which have expanded and are consequently at lower temperatures. With increasing frequency, the wavelength decreases; the temperature gradients are thus increased and the rate of flow of heat from a compressed region to the next rarefied one becomes greater. This contributes to an increase in the entropy of the system and thus gives rise to energy losses. In equation 1.5, α can then be written as

$$\alpha = \alpha_v + \alpha_t + \ldots\ldots$$

where α_v, α_t, etc. are respectively the co-efficients of absorption due to viscosity or damping, thermal effects, etc.[1.2]

Ultrasonic waves like optical and acoustic waves can be reflected, refracted and transformed in passing from one medium to another. They give rise to standing waves and can be diffracted. When a wave travelling through a medium impinges on a boundary between it and a second medium, part of the energy travels forward as one wave through

the second medium while the other part is reflected back into the first medium, usually with a phase change. The amount of reflection is determined by the specific acoustic impedance which is defined as the product of the density and velocity. The specific acoustic impedance of any medium is also equal to the mechanical impedance per unit area of cross-section of the medium. Strong reflections take place when transmitting from a liquid medium to either a solid medium or to air; but in the case of solids to solids, the use of thin films of couplants (e.g. liquids) minimizes reflection. [1.3]

Propagation of ultrasonic waves at angular incidence may result in wave transformation. A common example would be an S wave passing from a solid to a liquid and hitting the liquid at an angle. At the boundary between the two media, reflected L and S waves and transmitted L and S waves may form with different amplitudes and different angles of travel, depending on the angle of incidence of the original S wave and also on the impedance of the materials. But since liquids do not support the propagation of S waves, only the transmitted L wave and the reflected L and S waves remain. The transmission of ultrasonic waves through a liquid may result in cavitation of the liquid. This topic will be treated in detail in a later chapter.

1.3 PRODUCTION OF ULTRASONIC WAVES

Sonic energy is produced by the conversion of another form of energy and the means of doing this is normally referred to by the term "transducer". The type of transducer used depends on the conditions under which the ultrasonic wave is to be propagated i.e. in a gas, liquid or solid and also on the most suitable form of energy available for conversion into sonic energy. For practical purposes, the methods of production of ultrasonic waves can be

divided into three groups, mechanical, piezoelectric and magneto-strictive generators.

MECHANICAL TRANSDUCERS.

Mechanical generators fall into two groups - static and dynamic. Whistles or static generators utilise the fact that when high speed gas or liquid jet impinge on an obstacle or are directed into a resonant cavity, intense edge tones or oscillations at an ultrasonic frequency can be produced by suitable design of the whistle. The resonant cavity whistle by Galton is the oldest and Brown and Goodman [1.4] give a detailed account of the designs, operation and applications of the more recent types of whistles.

Sirens or dynamic generators are composed basically of a chamber covered with a disc or stator and a rotating disc or rotor. The stator and the rotor each contain a large number of holes, the number on the rotor being equal to that on the stator. On rotation of the rotor, holes are alternatively aligned and unaligned with the holes in the stator. Compressed air is continuously fed into the siren producing high pressure pulses of gas and a sound wave whose frequency depends on the speed of rotation of the rotor. Allen and Rudnick [1.5] designed a siren with a rotor of light alloy and high tensile strength, containing 50 to 300 openings and this rotates at a speed of up to 8,000 to 50,000 r.p.m.

PIEZOELECTRIC TRANSDUCERS:

In 1880, J and P Curie [1.6] found that a quartz crystal cut in a certain manner, developed equal and opposide charges on the opposite faces, with a consequential difference of potential; when these faces are subjected to pressures. This is the direct piezo-electric effect and has been observed in several other crystals such as tourmaline, Rochelle salt, etc. The theory of piezoelectricity and the manner in which piezoelectric cyrstals are cut with reference to their polar axes are given in detail by Mason.[1.7]

Lippmann (1881)[1.8] predicted the reciprocal piezoelectric effect which was later discovered by J. and P. Curie. According to this phenomenon, piezoelectric substances exhibit a change in size when an electric force is applied in the direction of the polar axis. When a potential difference, V, is applied to the opposite faces, the amount of expansion or contraction is given by

$$\delta x = \beta_1 V \qquad \text{(longitudinal effect)}$$

$$\delta x = \beta_2 V \frac{1}{d} \qquad \text{(transverse effect)}$$

where β_1 and β_2 are the piezoelectric moduli and d is the thickness of the crystal.

If an alternating electric field is applied in the direction of the polar axis, the crystals will expand and contract producing oscillations in the surrounding medium. The amplitude of the oscillations is a maximum when the electrical frequency is resonant with the fundamental frequency of the crystal and the waves produced are such that

$$d = \frac{\lambda}{2} = \frac{V}{2\nu}$$

where λ and ν are the wavelength and frequency respectively and d is the thickness of the crystal.

Most recently, barium titanate and some polycrystalline ceramics have been developed as transducers for ultrasonic waves and these are discussed in detail by Carlin [1.3]. In this case, prepolarization of the crystal is necessary since it does not have piezoelectric property as formed. This is done by applying an electric field of about 2,000 volts/cm of thickness across the crystal at temperatures above its Curie point (120°C). The resulting crystal has a lower electrical impedance than quartz and hence, the voltage which must be placed across it to make it operate is low.

Piezoelectric transducers convert electrical energy to mechanical energy and the design of the oscillatory circuit used to supply electrical oscillation to the transducer depends on the type of material used as a transducer, i.e. on the properties of the particular material. For example, barium titanate transduces operate at much lower voltages than quartz; and the exact control of frequency is not essential as with quartz crystals. Furthermore, the medium in which ultrasonic waves are to be propagated determines to some extent the type of circuit to be used. A circuit for the production of ultrasonic waves in air may be unsuitable for propagations in liquid media as the damping of the crystal stops the reaction.

The magnetostrictive transducer was used in the experimental work and a detailed description of it is given in Chapter 3 of this thesis.

1.4 APPLICATIONS OF ULTRASONIC WAVES.

Applications of ultrasonic waves can be divided into two basic classes : low and high intensity applications.

LOW INTENSITY APPLICATIONS:

The industrial applications of low intensity ultrasonic waves are considerable developments of the techniques used for measuring acoustic velocities and absorption. Velocity measurement methods have been adopted to such purposes as the location of defects in metals, thickness gauging, determination of elastic constants and estimating concentrations of solutions. Absorption measurement techniques are used in estimating degrees of hardness of metals, determining grain sizes in polycrystalline materials, measuring pressures of gases and distinguishing malignant from healthy tissue in living matter.

The use of ultrasonic waves for the detection of discontinuities in solid materials is based on the echo method. In general, longitudinal waves are used and where possible, the single probe pulse-echo method is employed. [1.9] It consists essentially of passing a pulsed beam of ultrasonic waves through the specimen from a reversible transducer placed on one surface; the beam being reflected from the opposite surface or a defect, back to the transducer. In the absence of any defect, two peaks A and B appear on the screen of an oscilloscope (Fig. 1.1); representing the instant of transmission of the pulse (A) and its return (B) after a single echo. Where a defect is present, some or all of the sound energy is reflected back to the transducer due to a discontinuity of characteristic impedance. Another peak, C, is then observed between A and B; the distance AC determining the depth of the flaw, and the height of the peak, C the extent of the defect. Crystalline transducers are normally used in flaw detection but the technique is more complicated than given above due to the practical difficulties of mounting the transducer, prevention of wear from friction between the surfaces of the crystal and the material under test, and the possibility that the specimen may not have two parallel surfaces.

Absorption measurement techniques have useful medical applications. They are rendered successful by the fact that the characteristic impedances and absorption coefficients of different parts of the human body, such as fat layers, muscles, bone, etc. vary significantly.[1.10] Therapy, diagnosis and biological measurements [1.11] are the fields that have been widely exploited. In general, the technique is similar to that of flaw detection, with frequencies in the low megacycle range and coupling achieved by the immersion technique.[1.12] Fig. 1.2 is the plan of a typical

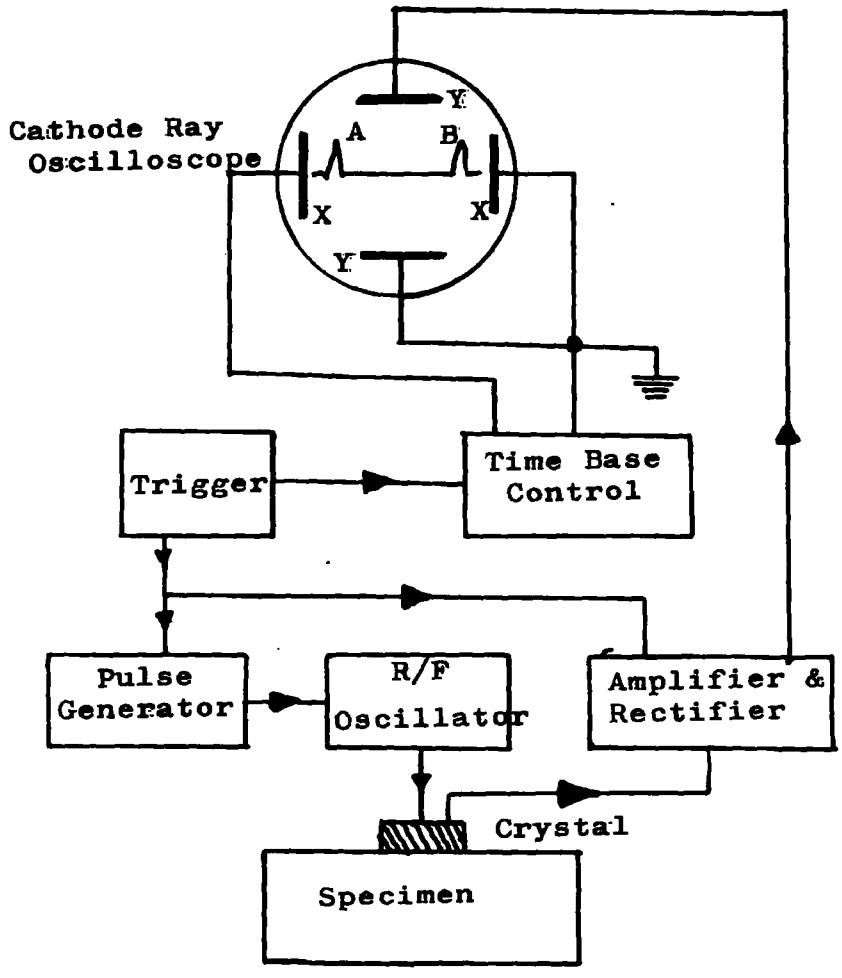

Fig.1.1 Block diagram of a flaw detector.

ultrasonic brain examination apparatus.

HIGH INTENSITY APPLICATIONS:

High intensity ultrasonic waves may be regarded as those for which there is no longer a linear relationship between the applied stress and the resultant strain. These waves have some effect on the medium through which they pass and these are utilised in metallurgy, chemical and biological applications, medical applications and cleaning.[1.13] Cavitation and agitation of the liquid may be involved in ultrasonic cleaning. The frequency range 20 to 40 kc/s, where cavitation effects are most pronounced, is most frequently used. Ceramic transducers can be used in cleaning but magnetostrictive transducers are often preferred because of their rugged nature and their ability to withstand rough handling. The work is immersed in a tank containing a liquid which is selected both for optimum cavitation conditions and its cleaning characteristics - detergent properties, ability to degrease, etc. Fig. 1.3 illustrates a conveyor belt system for cleaning a large number of components which are fed to the tank. Ultrasonic cleaning is especially useful where normal methods are either liable to cause damage, ineffective or laborious. Applications include removal of blood, etc. from surgical instruments after use; the cleaning of grease and swarf from small orifices in engine components and the removal of lapping paste from lenses after grinding, without scratching. [1.14]

Applications of high-energy ultrasonics to the treatment and working of metals have been very successful. They include drilling, treatment of melts, soldering and welding. Defects in metals caused by the oclusion of gases when a molten metal solidifies, can be removed by irradiating the molten metal with ultrasonic waves, under normal cooling conditions for the formation of crystals at the

temperature of solidification. The effect of high energy is to cause the crystals to be broken up by the action of cavitation. The yield is a solid of fine grain structure.

Ultrasonic soldering can be effected without the use of any flux and a consequent elimination of corrosive substances. The transducer is usually magnetostrictive and the soldering iron is similar in design to the ultrasonic drill, the essential difference being the electrically heated bit on the iron which replaces the tool at the end of the drill. Ultrasonic soldering has been most successfully applied in the soldering of aluminium and for "micro-joints".

High intensity ultrasonic welding has been carried out at normal temperatures and without any special surface preparation. The yield is practically undeformed, and it is suggested that the physical mechanism is that of molecular diffusion across the surfaces in contact with one another.[1.15] Other applications of ultrasonic waves include the use of liquid whistles in emulsification, dispersion, degassing, grain refinement; and chemical reactions. Chemical reactions are treated in detail under the effects of cavitation in Chapter 2.

CHAPTER 2.

2.1 CAVITATION.

A phenomenon that may feature in the propagation of ultrasonic waves through a liquid, and which is widely held to be responsible for some of the applications of high intensity ultrasonic waves in liquids, is cavitation. Cavitation may be defined as the formation, followed by a rapid collapse of small cavities or bubbles into a liquid phase. It can be produced not only by intense acoustic fields, but also, by other means such as heated wires, venturi tubes, high speed ship propellers, underwater sparks, rapidly rotating rods, etc. These cavities may contain air or vapour or may be almost empty. Cavitation will occur in a liquid when pressure is reduced to a certain critical value without change in the ambient temperature, or, conversely, when the temperature is raised above a critical value at constant pressure. Thus, in so far as the inception of cavitation is concerned, and from a purely physical-chemical point of view, there is no difference between boiling of a liquid and cavitation in a liquid.

The phenomenon of cavitation is complex and its study is complicated by the large number of factors that influence its production. For example, the pressure threshold of ultrasonic induced cavitation is influenced by local variations in liquids such as density, viscosity, surface tension, gas content of a liquid and in particular, the frequency of the acoustic wave. Basically, ultrasonic production of cavitation can be explained as follows :

The propagation of acoustic waves through a liquid results in the oscillations of particles of the medium, and, consequently, the formation of regions of compression and rarefaction (Chapter 1). The rarefaction region is associated with the existence of a negative pressure and, depending on the pressure of the acoustic waves and on the forces holding the liquid together, [2.1] cavities may be formed

as the liquid is then literarily "torn apart". Compression regions on the other hand, are regions of high positive pressures and the cavitation process is completed when the bubbles collapse in these regions. The entire process may or may not be completed during an acoustic cycle.

CAVITATION NUCLEI :

The micro-bubbles of cavitation are believed to be formed in the presence of weak spots or nuclei [2.2] in the liquid. These nuclei and weak spots act as centres of the bubbles. On the basis of physical arguments, it is unlikely that completely dissolved gases can play an important role during the inception process except in so far as nuclei that would not grow under reduced pressure because they are of too small a size, may reach critical growth size by prior diffusion of gas into the subcritical nucleus. While the presence of gas is probably essential, a complete explanation of the phenomena does not yet exist, although the rupture of liquids containing solid particle nuclei has been investigated. [2.3] More recently, both theoretical and experimental work has been carried out in support of the theory of nucleation process in cavitation. [2.4]

The reverse of nucleation also holds and it is possible to denucleate a liquid, thereby increasing its strength against cavitation. Sette [2.5] investigated the effect of cosmic rays as the origin of nuclei and also used gamma rays from ^{60}Co to irradiate water through which ultrasonic waves were propagated. His observations on the cavitation threshold for a water tank shielded and unshielded from the effect of these rays, confirm the ideas of denucleation and nucleation respectively. Exposure of liquids to high pressures [2.6] (about 1,000 kg/cm^2) also increases the strength of liquids against cavitation.

TYPES OF CAVITIES :

Figure 2.1 and Figure 2.2 illustrate two types of cavitation on the backs of marine propeller models. In Fig. 2.1, a fully developed cavity exists near the tip; and is termed a "steady" cavity. Cavities of this type can be observed in ultrasonically irradiated liquids when the acoustic field is weak. They are usually gas filled and large and the process corresponds to a quiet degassing due to the liberation of a certain amount of dissolved gas from the liquid. They do not produce any appreciable amount of noise and will remain in the liquid until they reach the surface by buoyancy. "Transient" cavitation is illustrated in Fig. 2.2 and has occurred in the form of discrete bubbles which grow in regions of low pressure and collapse as they proceed into high pressure regions. We shall be mainly concerned with the latter type in subsequent discussion.

Cavities may also be classed by the content of the bubbles. When water is irradiated with ultrasonic waves of the correct intensity for cavitation, three types of bubbles may be formed:- gas filled bubbles in which the dissolved gas in the liquid constitutes a high percentage of the bubble content; vapour filled cavities with little or no gas content; and empty cavities or voids.

GAS-FILLED CAVITIES :

Transient gas filled cavities are mostly observed when aerated water is irradiated. Under the correct conditions for cavitation onset, dense comet like streamers appear in the water, at short distances from the transducer face. The streamers contain a large number of small bubbles of various sizes which oscillate in a very turbulent area. The bubbles grow by the mechanism of "rectified diffusion" [2.7] whereby gas diffuses into the bubble form the water. This mechanism is explained thus :

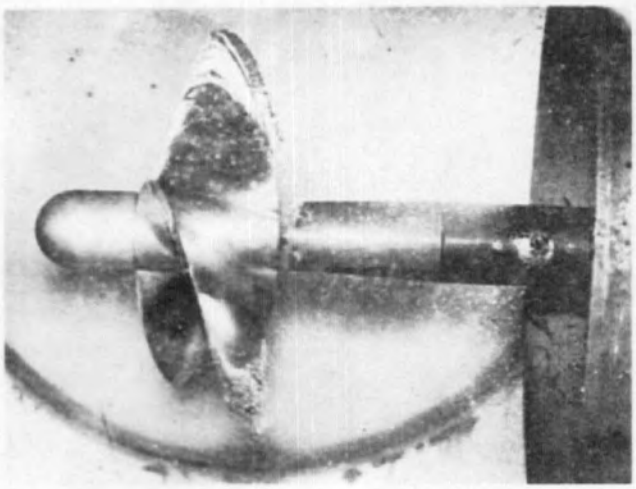

Fig. 2.1

A model propeller, showing "steady" cavitation near the tip of the uppermost blade.

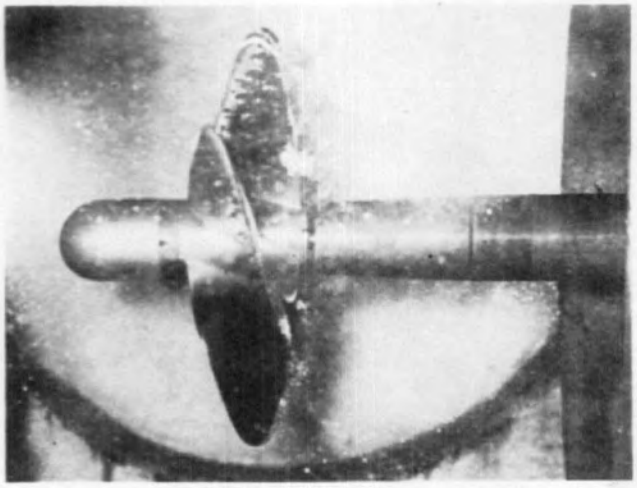

Fig. 2.2

Cavitation on a model propeller showing "transient" cavitation.

During the positive half cycle, the solution at the bubble interface is under-saturated and gas tends to migrate out, while the solution is super-saturated during the negative half cycle, producing a continuous excess of gas influx. Since the surface area of the bubble is larger during the later half cycle, there is a resultant diffusion of gas into the bubble. This growth process is a cumulative one, and requires that the acoustic excitation must exceed the threshold for growth and must also persist during a sufficiently long period in order to establish a steady state for cavitation.

During the growth process, some micro-bubbles will reach their "resonance size" i.e. the size at which their natural frequency equals that of the exciting acoustic field, and they will oscillate violently, consequently splitting into small bubbles. The natural resonant frequency of the small bubbles is higher than the exciting frequency of the acoustic field and they will in turn grow by gas diffusion.

In Fig. 2.3, five bubbles of decreasing sizes r_D, r_M, r, r_m and r_o which are submitted to an intense field of exciting frequency f_r and corresponding to the resonant frequency of bubble r_M are shown. r_D, with a lower natural frequency will grow by rectified diffusion and rise to the surface by buoyancy, while r_m will oscillate violently and split into medium sized bubble r_E (say) and smaller bubbles r_e(say). Bubbles r, r_m r_o and the resultants r_E and r_e of the splitting of r_M, will grow to collapse later.

This is also known as the "linear resonance of gas bubbles" and in the presence of very intense acoustic fields, the expansion phase (negative pressure) increases so rapidly that there is not enough time for diffusion of gas into the bubble and gas evaporation from the water proceeds more quickly.

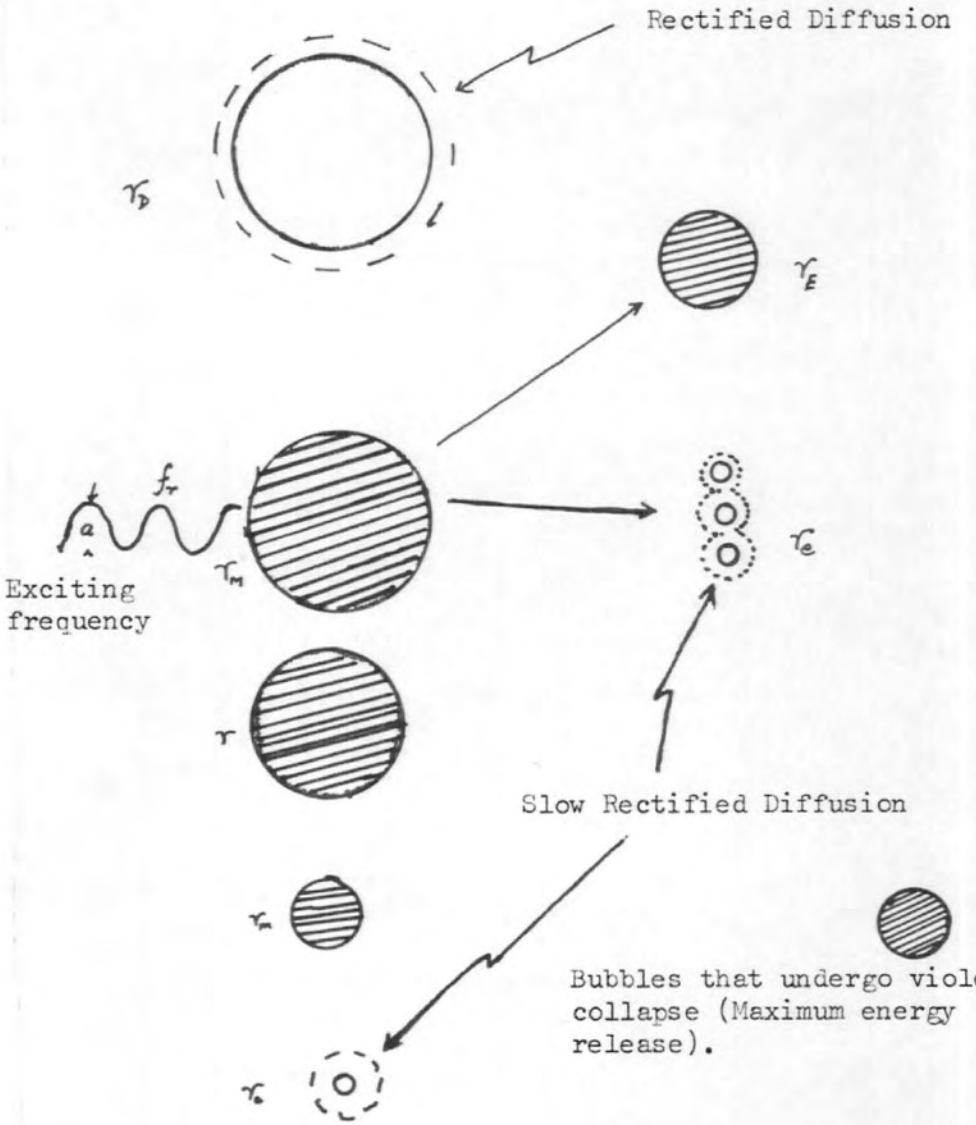

Fig. 2.3 Growth and Collapse processes of gassy bubbles.

f_r Natural resonant frequency of bubble r_M

a Amplitude of exciting sound wave.

VAPOROUS CAVITIES :

Gas filled cavities can be eliminated by using degassed liquids. The pressure threshold for cavitation in undegassed water is lower than that for degassed water. When thoroughly degassed water is irradiated, mostly vaporous cavities are observed. Vaporous cavitation is characterized by the appearance of a large number of micro-bubbles (transient cavities) throughout the entire mass of irradiated liquid. Their lifetime is shorter than that of gas filled cavities as they are generated and collapse in every acoustic cycle. Like gas filled cavities, vaporous cavities are formed during the negative half cycle but unlike gas bubbles, they do not undergo cumulative growth process but are compressed during the subsequent positive half cycle. This compression results in the condensation of vapour from the water/gas interface; the process taking place in two quick stages. First, the vaporous cavity is compressed isothermically at the temperature of the surrounding water, followed by an adiabatic compression in the last stage of collapse when the bubble wall acquires a high velocity. [2.8] This results in a violent collapse of the bubble walls and the production of powerful shock waves in the surrounding medium. These bubbles are only formed when the total negative pressure in the sound wave is equal to the sum of the cohesive pressure, the tensile strength and the ambient pressure; and they last for only an acoustic pressure cycle. [2.9]

VOIDS :

It has been mentioned that factors like viscocity, surface tension, etc. effect cavitation in liquids. Most viscous liquids have a high pressure and on the basis of H. Eyring's theory of viscosity, plasticity and diffusion, [2.10] natural holes can exist in a liquid into which molecules can move, leaving holes behind them.

This jump can occur when the molecule has accumulated enough heat energy to surmount an activation potential barrier and cavitation appears to be the result of coalescence of the natural hole in the negative pressure phase of the cycle. Cavities of this type are near-empty.

The onset of cavitation is often indicated by a hissing sound - cavitation noise - and the noise level increases as the input power to the transducer is increased. The cavitation noise spectrum consists mainly of a continuous background on which are superimposed a number of spectral lines corresponding to the exciting frequency and its harmonies. Noise level is a maximum at the resonant frequency of a transducer and this gives an indication of the correct frequency of operation. Cavitation is also accompanied by a weak emission of light and this is known as sonoluminescence [2.11]. It was first observed by Marinesco [2.12] and is believed by some investigators to be the result of gas incandescence; while others believe chemical luminescence occurs [2.13]. Apart from the rise in temperature of a liquid due to the absorption of acoustic energy, it is also believed that cavity contents attain high temperatures just before the collapse phase. The intense shock waves released on the collapse of cavities have been investigated widely and will be discussed in a later section of this chapter.

2.2 THEORETICAL CONSIDERATIONS.

One of the earliest theoretical considerations of cavitation was the Besant-Rayleigh problem which was an investigation into the behaviour of a spherical cavity in an incompressible fluid and in the presence of an alternating pressure. In his solution of this problem, Rayleigh [2.14] considered a bubble containing a permanent gas which he assumed to be isothermal. For a void of

initial radius r_o in a liquid of density p under a constant hydrostatic pressure P_o, he showed that at any subsequent time, when the radius had decreased to a value r, the pressure in the liquid is a maximum at a distance $4^{1/3}$ r and is given by

$$P = P_o(4)^{-4/3}\left(\frac{r_o}{r}\right)^3 \qquad 2.1$$

The time for complete collapse of the cavity is

$$t = 0.915\, r_o \left(\frac{P}{P_o}\right)^{\frac{1}{2}} \qquad 2.2$$

where P_o is in dynes cm^{-2}. Hence a cavity of diameter 0.01 cm in water at normal temperature and atmospheric pressure has a life time of 5μs.

Beeching, [2.15] in 1942, extended the above work, taking into account surface tension effects and the pressure of the liquid vapour in the cavity. A more elaborate calculation was given by Silver [2.16] in which he introduced thermodynamical considerations such as the heating of the vapour in the cavity by compression, with a subsequent loss of heat to the liquid. But it is thought to be of doubtful value due to some unjustifiable assumptions made in the calculation.

In 1948, Knapp and Hollander [2.17] used high-speed cinematography to trace the life history of a cavitation bubble and confirmed the existence of very large radial velocities and accelerations during the collapse period; the behaviour of the bubble being similar to that predicted by Rayleigh's treatment of the collapsing void. Plesset [2.18] developed an equation for the motion of a vapour-filled bubble in a changing pressure field and applied this to an analysis of Knapp and Hollander's experimental results. But Plesset in his calculation assumed that the pressure distribution was the same as that measured under non-cavitating conditions, while Rayleigh assumed a constant pressure.

Noltingle and Neppiras [2.19, 2.20] gave calculations for ultrasonic cavitation for a point in a medium where pressure changes are known and controllable. They assumed an incompressible liquid, a constant gas pressure in the bubble over its life cycle and an exactly sinusoidal applied ultrasonic pressure. The diameter of the bubble is also assumed to be always much less than the wavelength of the applied waves. For an ultrasonic pressure wave of amplitude P_o and frequency $^{w}/2\pi$, super-posed on a pressure P_A; the external liquid pressure at infinity can be written as

$$P = (P_A - P_o \text{ Sin } wt) \quad \text{at time } t.$$

The equilibrium pressure of a gas bubble of radius R_o at time $t = 0$ is $(P_A + {}^{2S}/R_o)$ where S is the Surface tension of the liquid; and the kinetic energy of the whole mass of liquid, density ρ, is $2\pi\rho R^3 \left({}^{dR}/dt\right)^2$. This energy can be equated to the algebraic sum of the work done by the surface tension, gas pressure and liquid pressure at infinity; giving as the energy equation :

$$\int_{R_o}^{R} \left\{ 4\pi R^2 \left[P_o \sin \omega t - P_A + \left(P_A + \frac{2S}{R_o}\right)\frac{R_o^3}{R^3} \right] - 8\pi RS \right\} dR = 2\pi\rho R^3 \left(\frac{dR}{dt}\right)^2 \qquad 2.3$$

if the gas changes are isothermal. Differentiating with respect to R, the equation of motion is

$$2R\left[P_o \sin \omega t - P_A + \left(P_A + \frac{2S}{R}\right)\frac{R_o^3}{R^3}\right] = 4S + 3\rho R\left(\frac{dR}{dt}\right)^2 + 2\rho R^2 \frac{d^2R}{dt^2} \qquad 2.4$$

Very high pressures and radial velocities associated with cavitation occur during collapse, when the walls of the bubble rush inwards until they strike the gas in the bubble. Since the total collapse time is a small fraction of the period of the ultrasonic vibration, P can be regarded constant for its duration and the surface velocity

of the bubble during the collapse is

$$V^2 = \frac{2P(\gamma-1)}{3\rho\gamma}\left[\frac{P(\gamma-1)}{Q\gamma}\right]^{\frac{1}{(\gamma-1)}} \qquad 2.5$$

if the gas changes are adiabatic, γ being the ratio of the specific heats for the gas and Q the pressure of gas in the bubble at its maximum radius.

So far, no account has been taken of any form of damping which, if considered, would have made the amplitude of the oscillations fall off rapidly as confirmed by the experimental work of Knapp and Hollander.

The bubble motion will be approximately simple harmonic if $P_o \ll P_A$, and the resonant frequency of the bubble, n, is given by

$$(2\pi n)^2 = \frac{3\gamma(P_A + 2S/R_o)}{\rho R_o^2} \qquad 2.6$$

In its growth, the bubble first attains a maximum radius, R_m, after which it starts to shrink and the pressure in the bubble at collapse is

$$p_{max} = Q(R_m/R)^{3\gamma} \qquad 2.7$$

It follows from 2.7 that the pressure in the resulting hydrodynamic shock wave increases with increasing R_m; and also that the larger the R_m, the lower the acoustic frequency and the greater the acoustic pressure. However, for a specific frequency, the pressure of the shock wave will increase with the acoustic pressure provided the total time of collapse of the bubble (τ) does not equal half the acoustic period [2.21](T), i.e. $\tau = \frac{1}{2}T$.

In 1964, G.A. Khoroshev [2.22] gave a theoretical treatment of the collapse of a cavity containing both air and vapour in the case of hydrodynamic cavitation. The mechanism of rectified diffusion [2.23]

has also been applied theoretically in the solution of the collapse of cavitation bubbles under conditions of liquid temperature sufficiently below the boiling point of the liquid and also in the neighbourhood of the boiling point. However, these treatments of cavitation bubble collapse are mostly for spherical bubbles but the chances are that the bubbles may not be entirely spherical during their life time.

2.3 MEASUREMENT OF THE RELATIVE INTENSITY OF CAVITATION.

Most applications of high intensity ultrasonic waves in liquids can only be accomplished under cavitation conditions. They include ultrasonic cleaning, chemical effects, etc. (Section 2.1). The results of cavitation can also be very destructive to an adjacent solid material as is the case with ships propellers and hydraulic systems. These solid materials undergo erosion after a long exposure to cavitation. These two effects of cavitation - erosion and ability to promote chemical reactions - are most commonly applied in the measurement of the relative intensity of cavitation.

CHEMICAL METHOD:

Ultrasonics effect chemical changes which are generally attributed to cavitation and most of these changes cannot be accomplished in any other manner. These effects include the speeding up of iodine reaction, oxidation, decompostion and crystallization.[2.24] The liberation of chlorine from carbon tetrachloride and of iodine from potassium iodide are the two chemical effects most commonly employed in cavitation intensity measurements. Satisfactory proportions for the latter solution are 20 ml of IN KI and 1 ml of one per cent starch solution to give a marked coloration. Free iodine yield can be greatly increased by the addition of 1 ml. of carbon tetrachloride. During irradiation, iodine is liberated and it reacts with the starch solution to give a blue colouration. The addition of

$^{N}/100$ sodium thiosulphate (about 0.1% of the volume of the mixture), causes the blue colour to disappear and on a second irradiation, the colour reappears and hence, the rate of iodine liberation can be calculated.

The second reaction used in intensity measurements is the free chlorine yield from a saturated solution of carbon tetrachloride in water. The indicator of free chlorine radical is a solution of ortho-tolidine reagent and the intensity of cavitation may be expressed as the optical density i.e. the negative logarithm of the fraction of light transmitted by the yellow solution resulting from the irradiation. This method will be dealt with in detail in a later chapter.

Both reactions are attributed to the presence of activated oxygen, the series being as follows :-

$$O_2 \longrightarrow O + O$$

$$CCl_4 + H_2O \longrightarrow Cl_2 + CO_2 + 2HCl$$

$$2HCl + [O] \longrightarrow Cl_2 + H_2O$$

The free chlorine then reacts with ortho-tolidine reagent to give a yellow coloured solution or in the case of potassium iodide :

$$2KI + Cl_2 \longrightarrow 2KCl + I_2$$

EROSION METHOD :

The use of cavitation damage processes as a means of measuring the relative intensity of cavitation can be grouped under the headings of soil removal and erosion. Soil removal consists of exposing test samples with soil coatings to cavitation under given conditions and measuring the amount of soil removed. A refined technique is based on the use of radioactive tracers which makes it possible for the initial degree of contamination of the samples to

be measured accurately. A standard sample would be a coating of a mixture of P^{32} with an appropriate soil, the amount of radioactive tracer being measured with a suitable Geiger counter or scintillation counter assembley before and after exposure to ultrasonic irradiation in a liquid.

Erosion techniques offer a most reliable method of measuring the cavitation in a liquid, and samples most commonly used are aluminium, tin or lead plates. When exposed to cavitation, the samples are pitted due to the implosion of cavitation bubbles and if the amount of pitting is assumed proportional to the cavitation taking place, the qualitative assessment of cavitation is available. [2.25] Quantitatively, the loss in weight of the metal samples offer an indication of the amount of cavitation taking place. More details about the samples and the method of estimation of cavitation activity by the erosion technique will be discussed in a later chapter.

FACTORS THAT INFLUENCE RESULTS:

There is some doubt as to which aspects of cavitation are responsible for erosion and chemical reactions. Opinions advanced are: (1) temperature rise, (2) pressure changes, or intense shock waves (3) electrical phenomena, (4) separation of water into ions, and (5) internal resonance. [2.26] Furthermore, a number of experimental conditions when varied, will affect the results. These include frequency, time duration, temperature, pressure - both acoustic and loading, etc.

It is accepted by most experienters that frequency does not effect ultrasonically induced chemical reactions except in so far as cavitation itself is frequency dependent. The effect of intensity changes on chemical reactions is illustrated in Fig. 2.4a and it can be seen that these reactions do not occur at low intensities. They appear at the threshold of cavitation and increase approximately linearly with increase in intensity. Iodine yields appear to increase with duration of exposure and this is shown in Fig. 2.4b. Cavitation

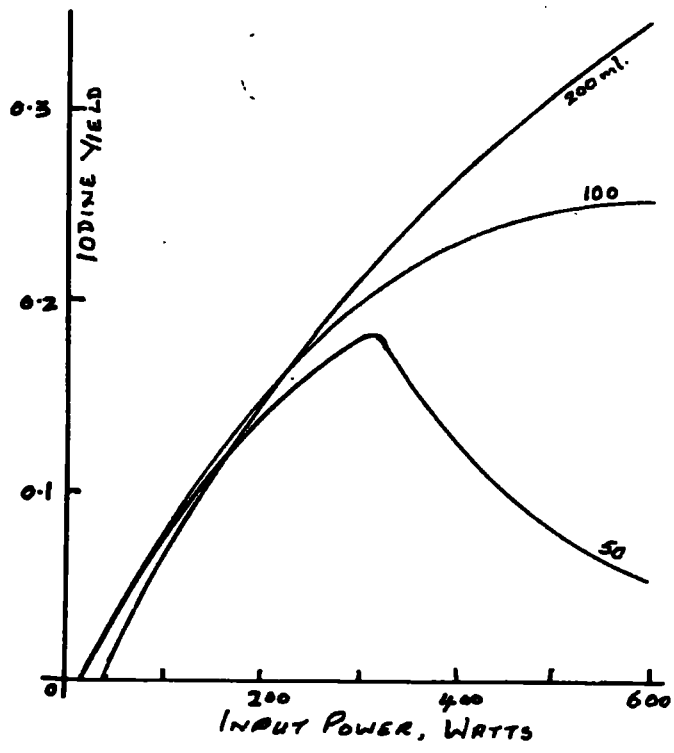

(a)

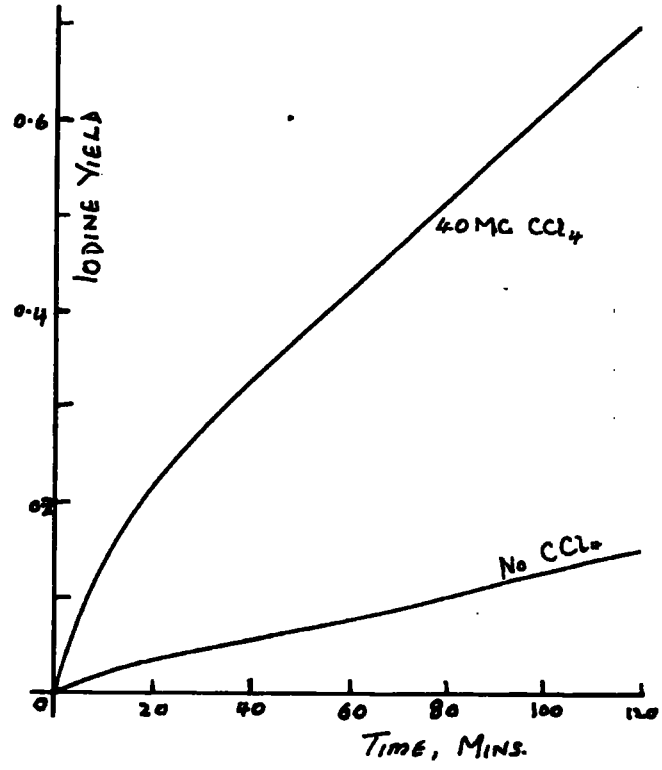

(b)

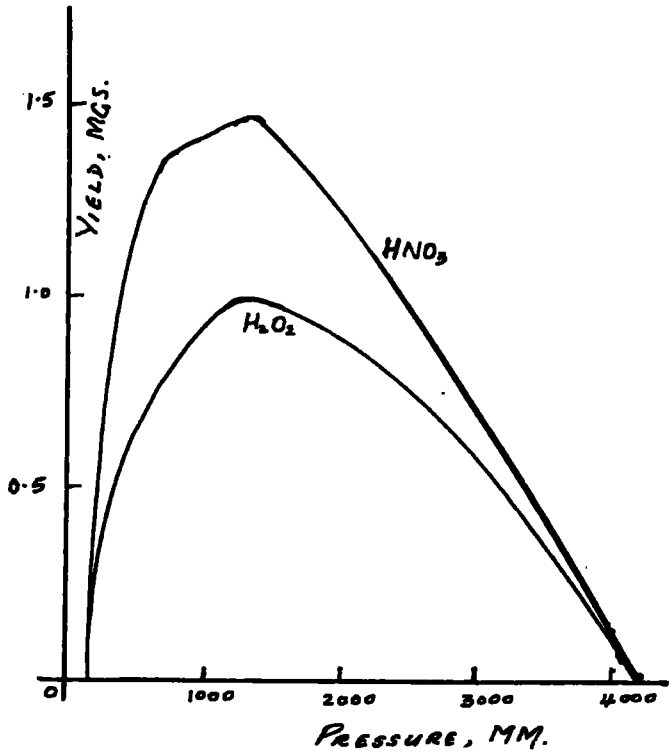

(c)

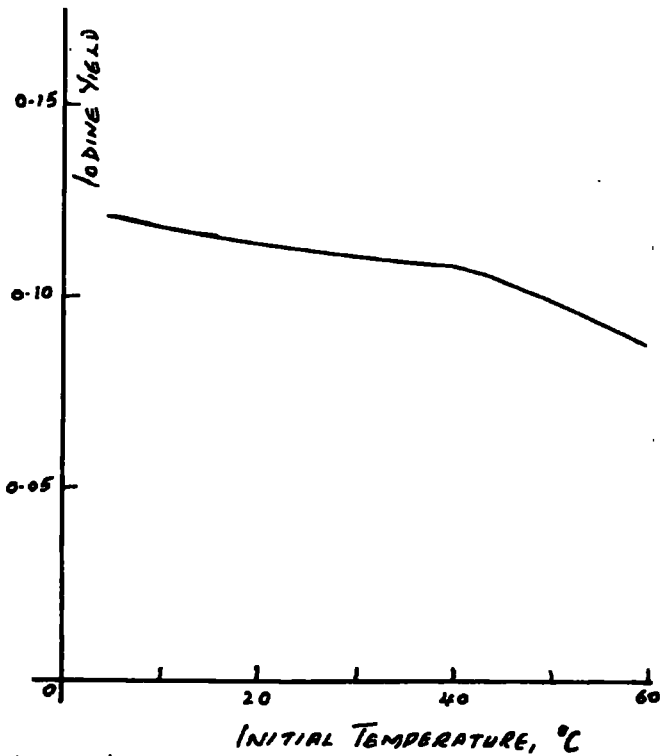

(d)

Fig. 2.4

Effect of various factors on iodine yield.

is a function of pressure and effect chemical reactions; but above 1,500 mm Hg., the pressure is too great to allow bubble formation (Fig. 2.4c). Temperature control during ultrasonic irradiation is difficult and it is known that yields are effected by temperature changes (Fig. 2.4d).

There is no clear description of the process that takes place during cavitation damage although a variety of postulates have been put forward. The phenomenon is a complex one involving many variables and as such, a coherent account is still not possible without assuming a priori that the mechanisms of importance are known. Factors of importance are the fluid dynamical, the electrochemical and the metallurgical aspects of corrosion.[2.27] Theoretical and experimental postulates have been put forward in support of a mechanical damage hypothesis for erosion. In general, it is agreed that the shock waves formed when cavitation bubbles collapse play an important part in erosion.

The nature of the damage is so intimately related to the response of the materials to impingment attack versus chemical activity that it is difficult to separate the effects. Thus, for long periods of exposure to cavitation pressure, inert materials show only plastic deformation while materials that react rapidly in corrosive media will yield corrosion products upon exposure. Relatively ductile materials show an "incubation" period during which plastic deformation occurs and no material is lost from the specimen. Nickel shows the formation of microscopic "hills and valleys" on its surface when exposed to cavitation; stainless steel shows slip lines and zinc monocrystal shows the hexagonal structure of the crystal.[2.28] Fig. 2.5 is an illustration of the "incubation" period for brass and four types of stainless steel.

Variations in the physical and chemical properties of the liquid medium complicate the study of cavitation damage mechanism. Factors,

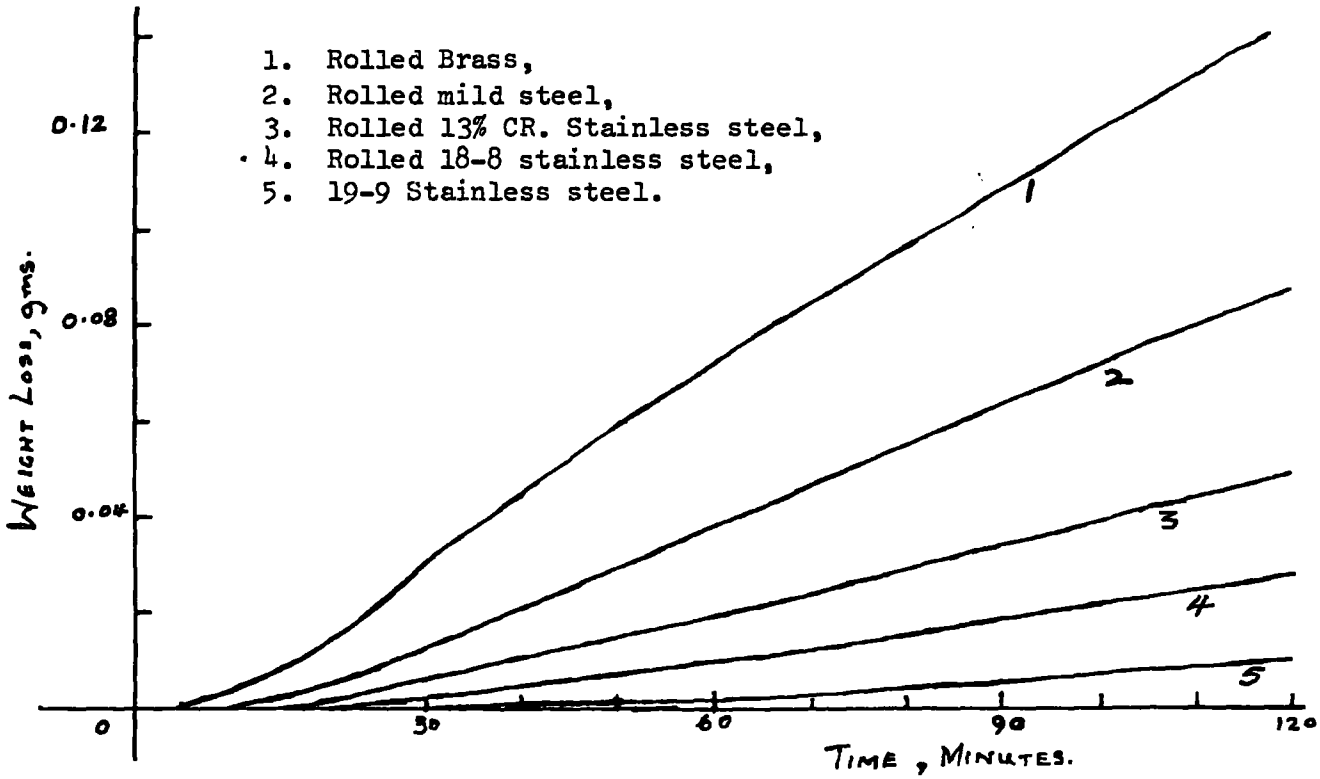

Fig. 2.5.

"Incubation Period" illustrated in tests of accelerated cavitation damage.

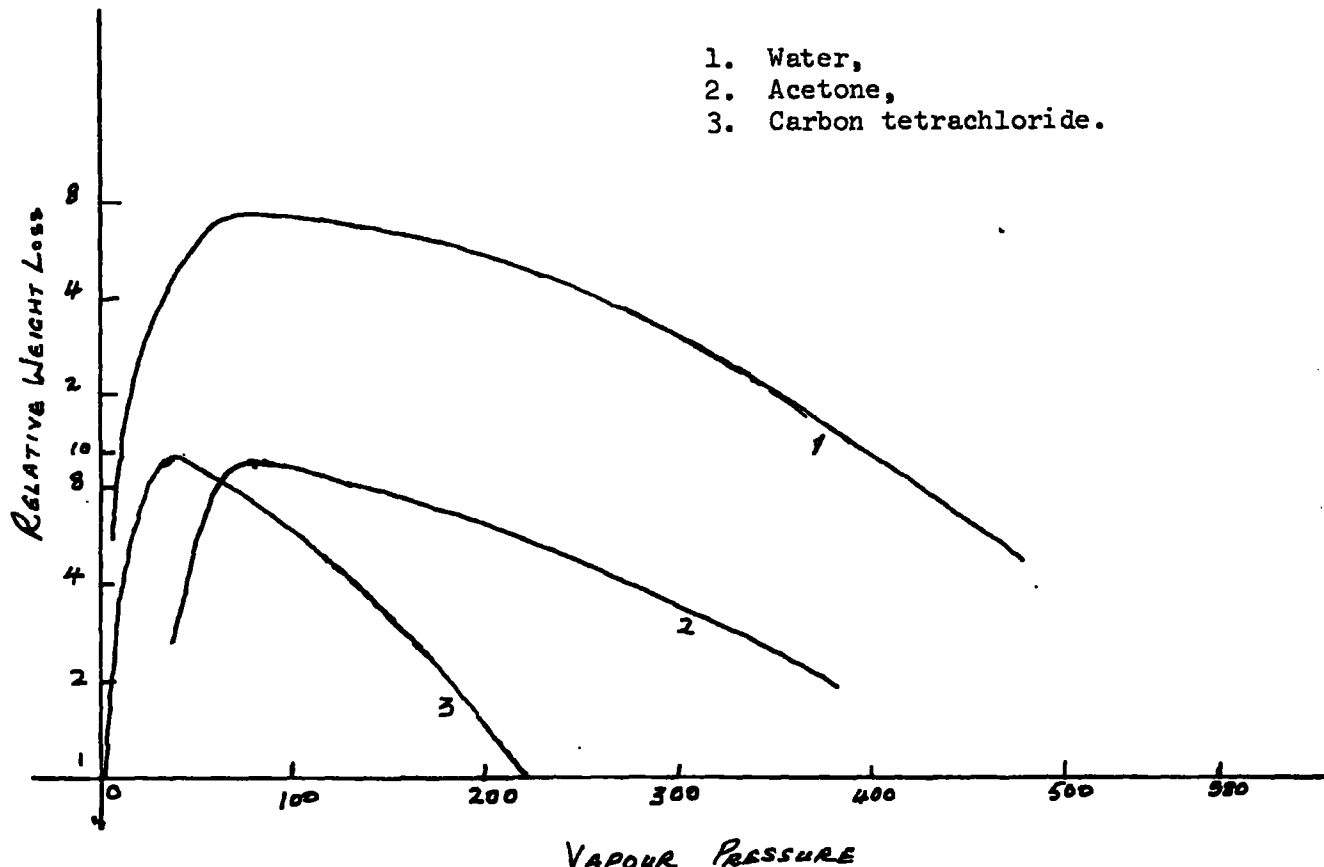

Fig. 2.6

Dependence of cavitation damage on saturated vapour pressure.

such as temperature, vapour pressure, gas content, surface tension, viscosity, compressibility and density effect results of cavitation damage.[2.29] The behaviour generally observed in examining the effects of the vapour pressure of the liquid on the damage process is shown in Fig. 2.6; the observed peak being associated with the vapour pressure and gas content. Since the collapse pressure would be higher for higher surface tension, other factors remaining constant, an increase in damage with increasing surface tension should be observed, (Fig. 2.7). Experimental results also show that cavitation damage decreases with increasing viscosity and this is shown in Fig. 2.8. Wilson and Graham [2.30] have also shown that cavitation damage should increase with increasing density and decreasing compressibility (Fig. 2.9).

In general, no single method of measuring the relative intensity of cavitation already discussed can provide results to better than $\pm$ 10%. Other methods suggested for the determination of cavitation activity are based on cavitation noise [2.31] or the production of sonoluminescence.[2.32]

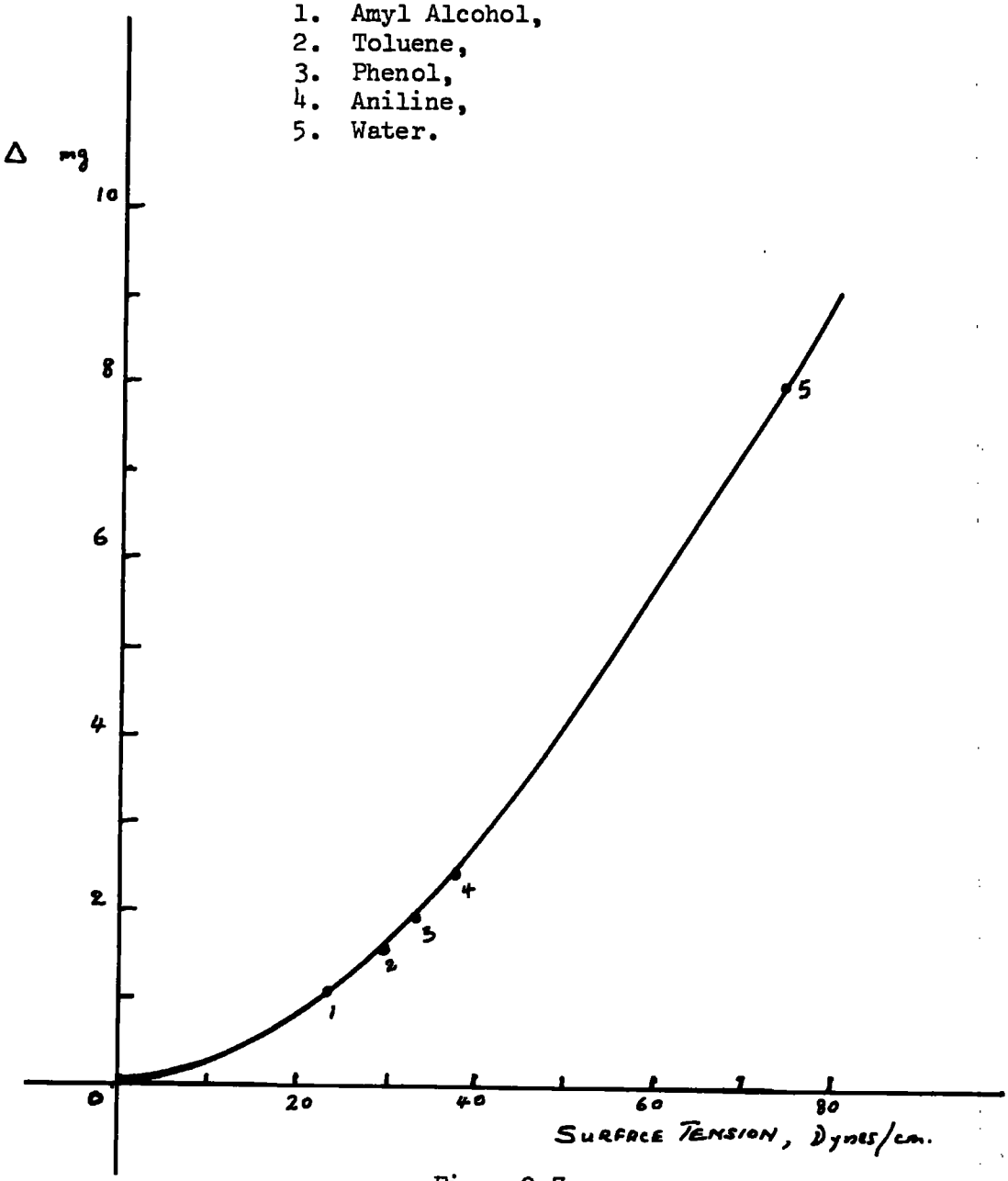

Fig. 2.7

Cavitation erosion as a function of surface tension.

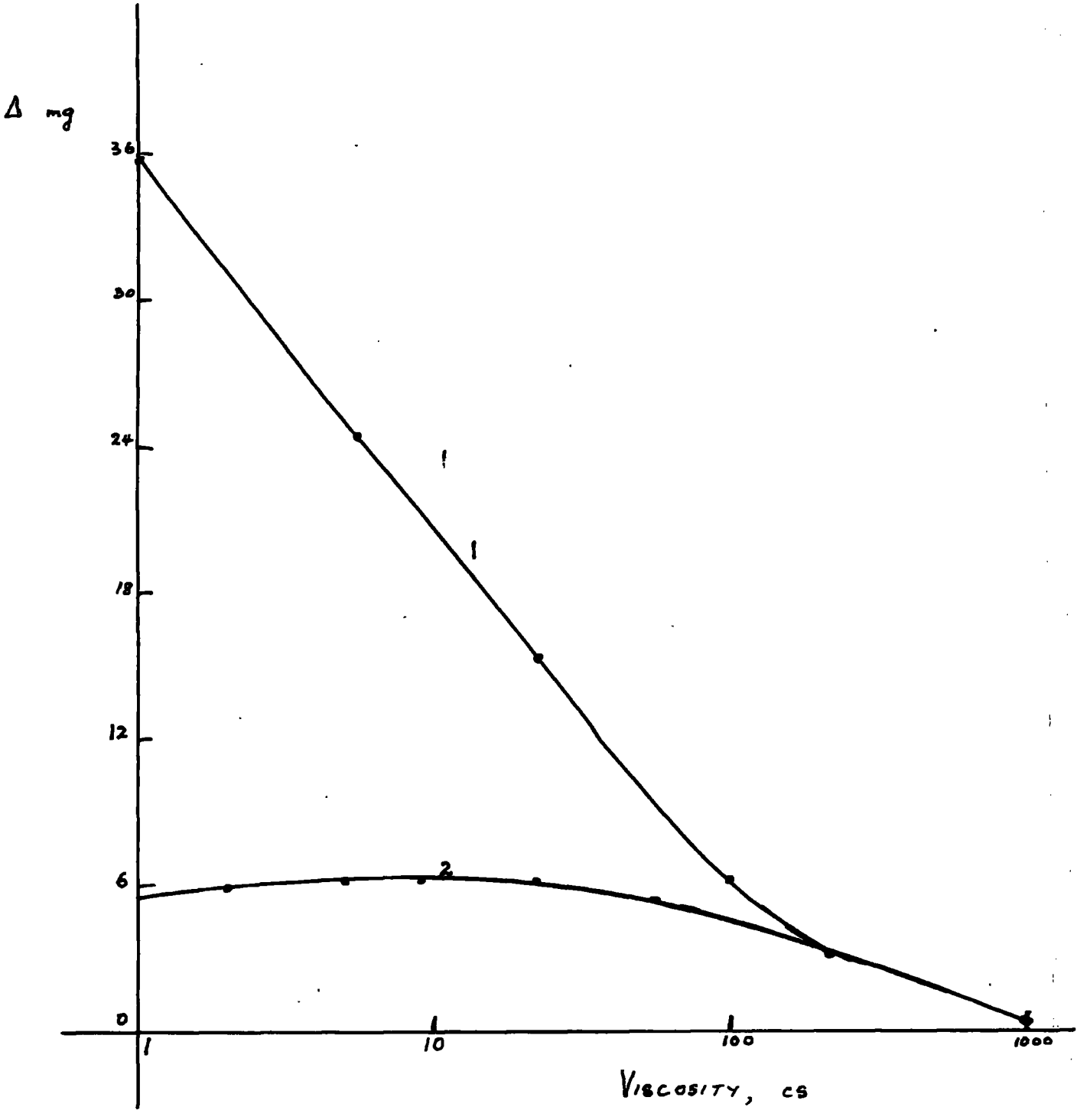

Fig. 2.8

Dependence of cavitation erosion on viscosity of liquid for (1) silver-plated and (2) aluminium samples.

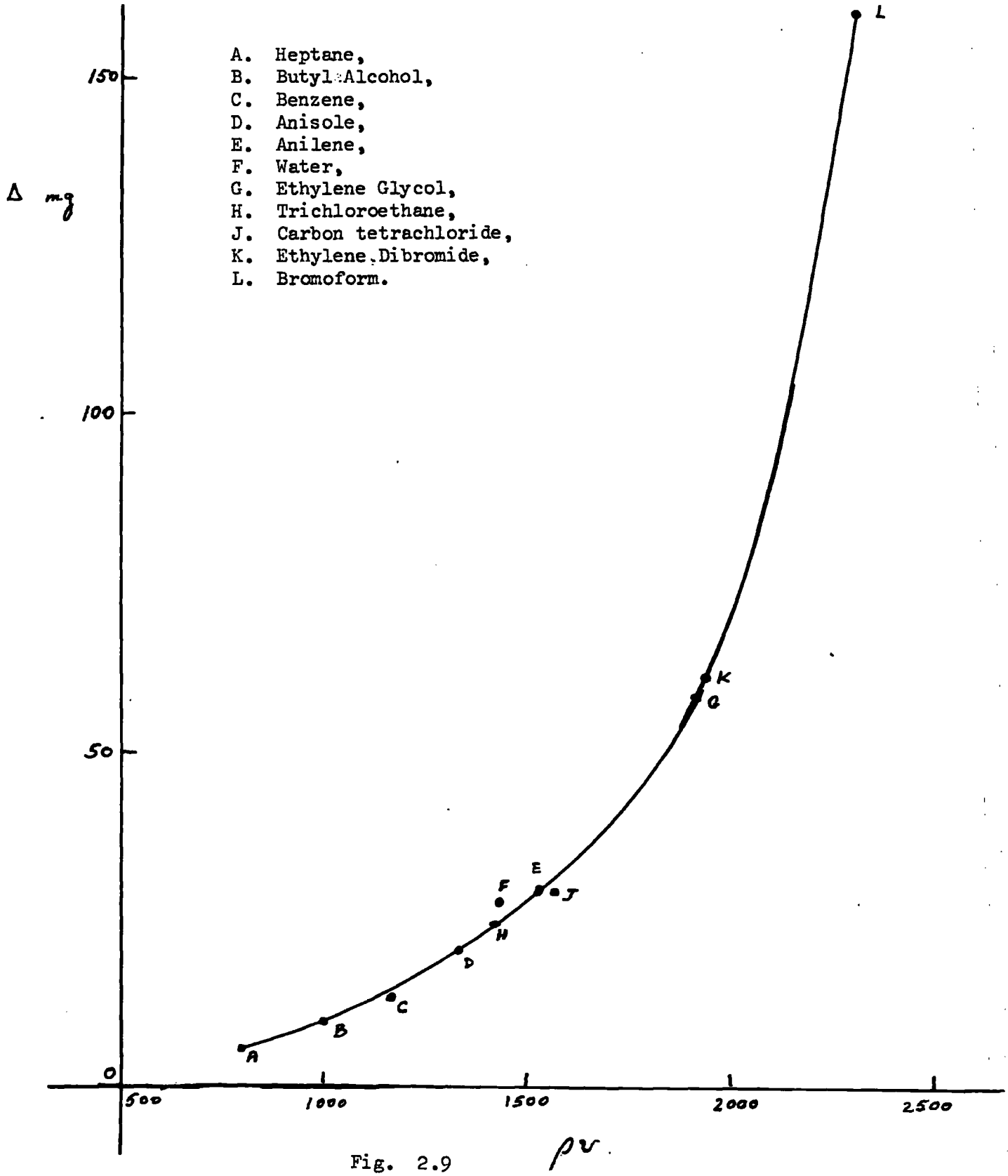

Fig. 2.9

Cavitation erosion as a function of the product of liquid density and sound velocity.

CHAPTER 3.

3.1 MAGNETOSTRICTION.

Magnetostriction [3.1] can be explained by the consideration of the Domain Theory. The fundamental magnetic particle in an atomic system is the orbital electron and in most systems, their magnetic effects nearly neutralize each other. However, in ferromagnetic materials, an exchange force exists that causes the atomic magnetic fields within a volume of 10^{-8} or 10^{-9} to lie parallel. These domains are each magnetized to saturation, their magnetic field directions being randomly alligned in any one of a number of fixed directions known as "directions of easy magnetization". In the presence of an external magnetic field, domains nearly parallel to the field direction grow in size, taking over the other differently orientated domains. This process continues as the strength of the external field is increased, until, each crystal of the material becomes one large domain. Further increases in the external field strength cause the domain in each crystal to rotate until it is parallel to the field direction. Externally, the material expands or contracts as the domains rotate.

When the domains are all aligned in the direction of the external field, the dimensional changes in the material cease and the latter is said to be saturated. The changes in dimensions are small, the relative deformation being of the order of 10^{-6} to 10^{-4}. Fig. 3.1 is an illustration of the magnitudes and signs of the magnetostrictive effects for nickel and cobalt.[3.2] All magnetic properties cease at the Curie point; but this is relatively high for all materials used in the construction of magnetostrictive transducers.

3.2 MAGNETOSTRICTIVE TRANSDUCER

The production of ultrasonic waves by the magnetostriction effect is accomplished by the conversion of electrical energy to sonic

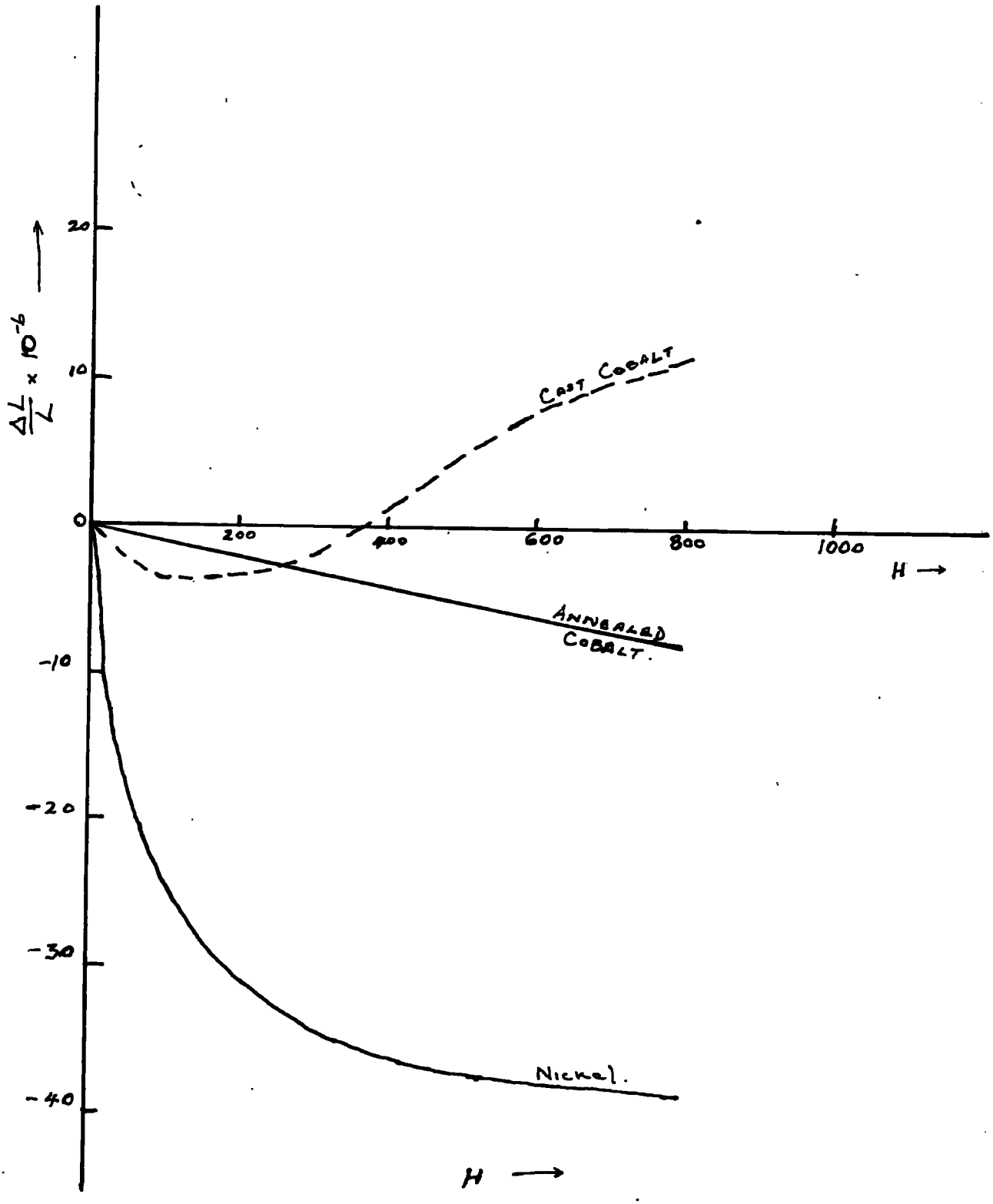

Fig.3.1 Relative deformation ($\Delta L/L$) as a function of field strength for nickel and cobalt.

energy. The magnetostrictive transducer is placed in an external magnetic field which is varied at an ultrasonic frequency to produce mechanical vibrations of the transducer. Normally, the material of the transducer is surrounded by a coil through which a high frequency oscillating current superimposed on an initial magnetizing current, is passing. The idea of the initial magnetizing current is to overcome the production of two directions of easy magnetization in the material by the oscillating magnetic field, which would have resulted in an average zero deformation of the material. Initial magnetization also causes the frequency of vibration of the deformation to be the same as the frequency of the oscillatory current.

In practice, the initial magnetization is produced either by the use of a permanent magnet or by passing a direct current through a coil around the material. The later is referred to as the D.C. polarising current and by the use of a choke-capacitance coupling to separate the d.c. from the oscillatory current, the two currents are passed through the same coil. For a maximum amplitude of vibration of the rod, the magnetostrictive transducer is operated at its natural frequency. This is accomplished by tuning the oscillatory current and hence the magnetic field vibration to be the same as the natural frequency of the rod. In this case, the rod oscillates freely, the vibrational amplitude is large and the relative deformation can be as much as 10^{-3}. Furthermore, the length of the rod is equal to a half wavelength of the sound radiated by it and can be represented by

$$\nu = \frac{V}{2\ell} \qquad 3.1$$

where V is the velocity of sound in the material and ℓ is the length of the rod.

Any material used as a magnetostrictive transducer must possess the following characteristics: (1) a high rate of change of magnetostriction with magnetic field, (2) High Curie temperature, (3) Good mechanical properties, and (4) Good corrosion resistance depending

on the condition under which the transducer is to be used. In addition, the heat dissipation in the material, the geometrical construction of the transducer and the strain that the material can withstand help to determine the performance of a transducer.[3.3] The level of operation of a transducer is determined by the heat losses due to eddy current and to mechanical and magnetic hysteresis.[3.4] It follows therefore that the removal of heat dissipated in the transducer by cooling is important and that the geometrical construction will affect the efficiency, the mechanical Q factor (Chapter 1) and many other factors.

The shape of a magnetostrictive transducer is often determined by: (1) the elimination of losses in the core material and (2) the desire to control the shape or field pattern of the transmitted beam. The shape or field pattern is in turn determined by the use for which the transducer is intended.

TYPES OF MAGNETOSTRICTIVE TRANSDUCERS:

Fig. 3.2 is an illustration of the shapes of transducers. The simplest type is the single rod transducer used for low power irradiations. Power losses in the material and the shielding of the interior of the material from the alternating magnetic field due to eddy currents impose practical limitations. Losses due to the interior of the material are eliminated by the use of a tube of the material and when slit tubes are used, eddy currents are eliminated. The disadvantages of the slit tube are a reduction in the cross-sectional area of its face and a slight variation in the frequency of operation (Equ. 3.1). These disadvantages are overcome by the construction of the laminated bar transducer fabricated of thin sections electrically insulated from each other. Each lamination acts as though it were exposed independently to the exciting field

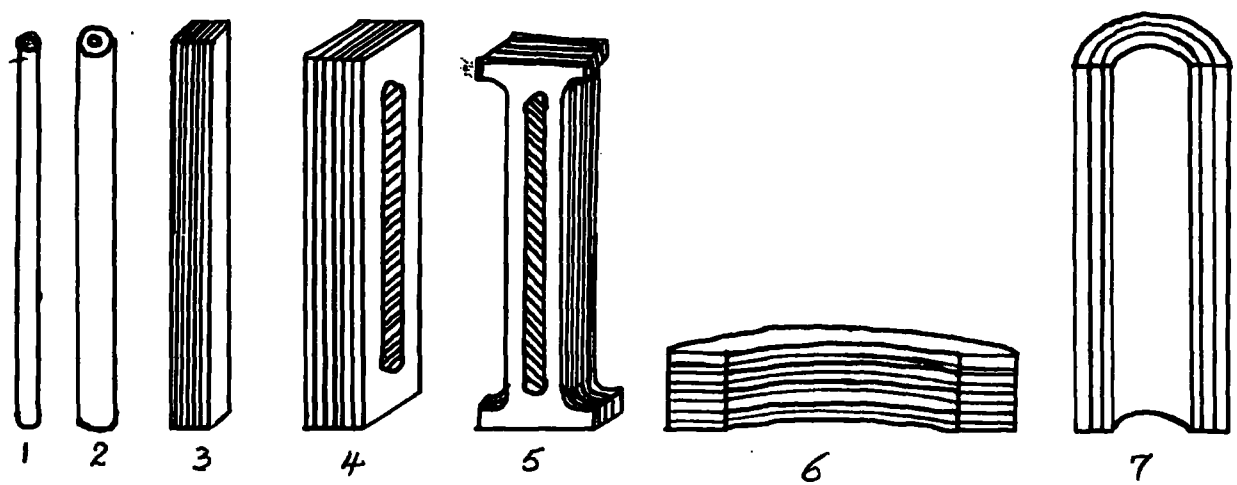

Fig. 3.2

Shapes of magnetostrictive transducers: 1. the single rod, 2. the tube, 3. the laminated rod, 4. Laminated rod with slot, 5. Laminated window type, 6. Laminated ring (cut away), 7. Laminated cylinder.

and they are bonded together with araldite or some other non-conducting layer in such a manner that they vibrate in unison. The thickness of the laminations affect the frequency response of the transducer and usually about 0.015 in thick is used below 30 kc/s; and about 0.05 in for higher frequencies.

With increasing frequency of operation, the length of the transducer decreases and hence its length to diameter ratio.[3.5] There are also magnetic flux losses [3.6] at the end faces but these defects are overcome by the use of the slotted bars or the window type transducers. Ring or cylindrical transducers are made with toroidally wound rings with laminated cores. Generally, they produce radial vibrations but when excited as a tube, they will radiate from the ends. The sensitivity of magnetostrictive properties such as permeability, saturation magnetostriction, etc., which depend on the internal structure of the material,[3.7] can be controlled by mechanical operations on the material and heat treatment. It is therefore important to anneal transducer materials.[3.8]

EQUIVALENT CIRCUIT OF A MAGNETOSTRICTIVE TRANSDUCER:

In general, an electromagnetic system can be described by the following equations :[3.9]

$$V = Z_o I + Z_{em} U \qquad 3.2$$

$$F = -Z_{em} I + Z_m U \qquad 3.3$$

where V is the voltage applied to the transducer and I the resulting current. Z_o, and Z_m are the 'clamped' and mechanical impedances of the transducer; U is the velocity of the transducer face, F the force applied by the face and Z_{em} the electromechanical transformation factor i.e. $Z_{em}U$ is the e.m.f. arising from a face velocity U.

For a rod-shaped transducer of length ℓ, cross sectional area

S, surrounded by an energizing coil system of n turns per unit length, equations 3.2, 3.3 become

$$V = Z_o I + (4\pi\lambda\mu nS)U \qquad 3.4$$

$$F = -(4\pi\lambda\mu nS)I + Z_m U \qquad 3.5$$

where λ is the magnetostrictive constant and μ is the effective dynamic permability.

Comparing equations 3.2 and 3.3 with equations 3.4 and 3.5, we have

$$(Z_{em})^2 = \left(\frac{L\lambda}{\ell n}\right)^2 \qquad 3.6$$

where $L = 4\pi n^2 S\mu\ell$ is the inductance of the system, neglecting eddy current and hysteresis losses.

The equivalent lumped constants are (Ch. 1):

$$M = \frac{\rho S\ell}{2} \; ; \quad \frac{1}{C_m} = K = \frac{\pi^2 SE}{2\ell} \; ; \quad Z_w = 2S\rho_1 v_1$$

where E is the effective Young's modulus, Z_w is the mechanical impedance of the medium, ρ_1 and v_1 are the density and ultrasonic velocity of the medium.

The equivalent electronic representation of the transducer[3.9] will then be as shown in Fig. 3.3, where,

$$L_2 = \frac{(Z_{em})^2}{K} \; ; \qquad C_2 = \frac{M}{(Z_{em})^2} \; ;$$

$$R_i = \frac{(Z_{em})^2}{R} \; ; \text{ and } \quad R_r = \frac{(Z_{em})^2}{Z_w} \; ;$$

L_2, C_2 and R_2 representing the stiffness, mass and the inverse damping of the vibrator respectively. R_2 is a combination of two resistances, R_i for internal motional losses and R_r for radiation losses. L represents the inductance of the core and windings and r the core losses.

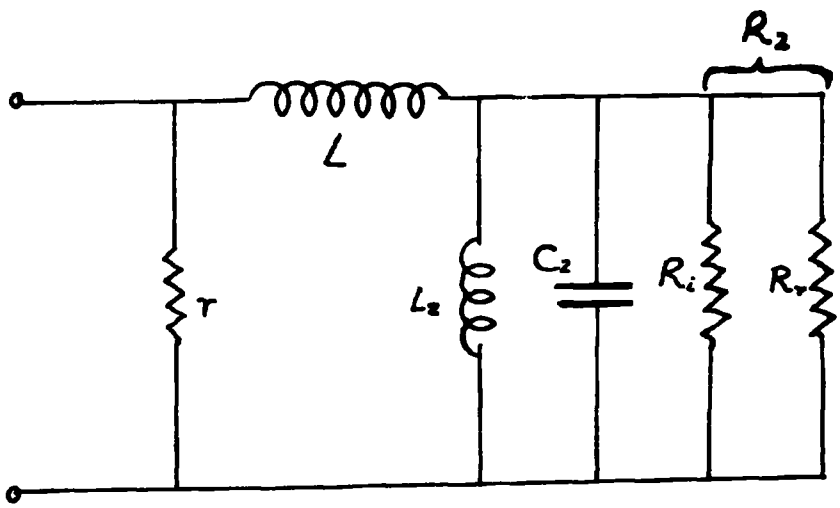

Fig.3.3. The Equivalent circuit of a magnetostrictive transducer.

3.3 POWER SUPPLY FOR MAGNETOSTRICTIVE TRANSDUCERS.

Electronic generators used with magnetostrictive transducers have the task of converting the mains frequency of the locality into electrical oscillations of high frequency suitable for operating the transducer. The level of sonic energy required and the radiation area of the transducer determine the size and power output of the oscillatory generator. Generators can be of two types :

(a) Mechanical or rotary generators,

(b) Valve generators.

Rotary generators [3.10] are used under arduous working conditions as exist inside a steel works. It consists essentially of the pre-magnetising unit, an accessory switch panel, the control portion and a rotor which is vertically mounted. The generator which is equipped with lubricated roller bearings, is water cooled and the entire unit is supported on anti-vibration mountings.

Valve generators are used in most ultrasonic applications and there are basically two types :

1. Power oscillator operating class C
2. Oscillator-Power amplifier with power amplifier operating class AB2.

A practical magnetostrictive oscillator of the first type is shown in Fig. 3.4. It utilises a push-pull oscillator system with the grid-cathode circuit comprising the oscillator proper and the output transformer in the plate circuit. Frequency control is effected by the choice of values for the tuning capacitors and by moving the two coils in the grid circuit with respect to one another. The number of turns on the output transformer sets the output impedance and a separate d.c. polarising current is fed in parallel to the transducer itself.

The oscillator-power amplifier type is often constructed in sections. Here, the frequency is determined by a self excited

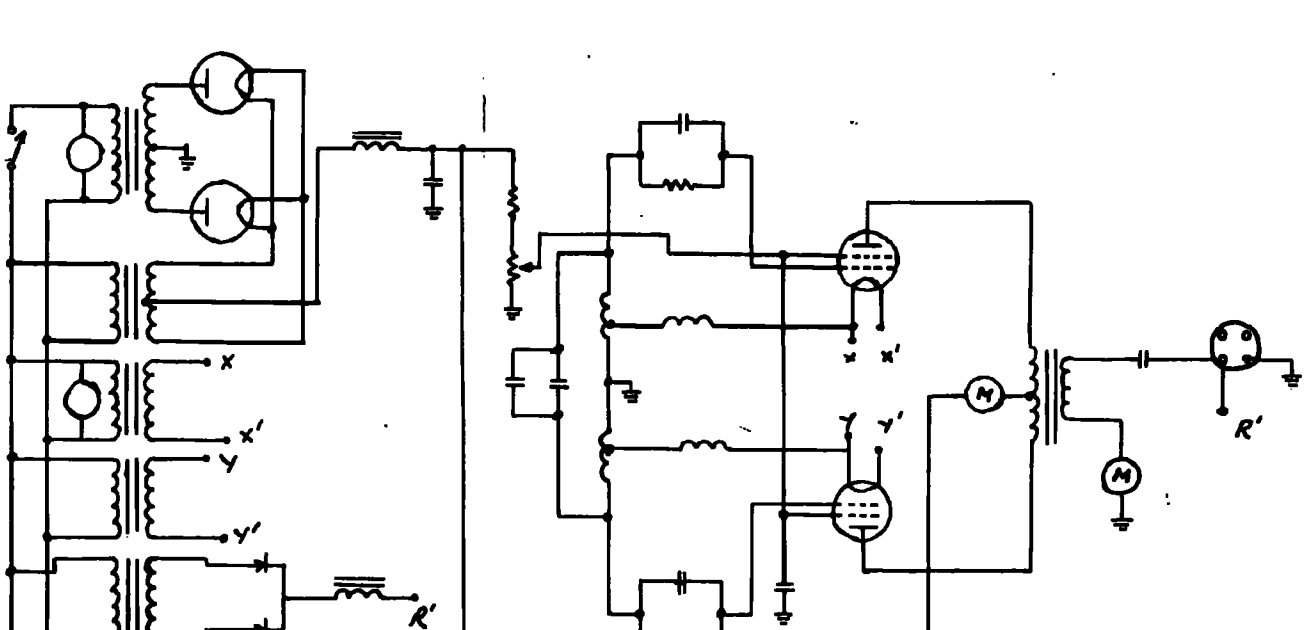

Fig. 3.4

A Typical Oscillator for driving magnetostrictive transducer unit.

oscillator which can be a variable frequency Wien bridge oscillator. In this way, the frequency stability of the generator depends on the oscillator. Stability is only achieved at low power delivery and consequently, voltage and power amplfication is necessary. A block diagram of this type of generator is shown in Fig. 3.5.

The aim of the research project required that this generator should supply high intensity oscillatory current at an ultrasonic frequency to a magnetostrictive transducer. Neppiras and Noltingk have shown that the forces of cavitation increase with decreasing ultrasonic frequency. Brown has also shown that cavitation intensity is directly proportional to the ultrasonic power output. In keeping with these conditions, it was decided to produce ultrasonic waves by supplying continuous electrical oscillations at a frequency of 20 kc/s, from a suitable generator (Fig. 3.6) with a variable power output, to a magnetostrictive transducer. It has a maximum input power of 4.0 kVA and a variable output power of up to 2.0 kW. Three output tappings are provided so that three transducer units can be driven, either separately or simultaneously.

THE GENERATOR:

The construction of the generator (Fig. 3.5) is in four sections which are numbered from the top. In chassis 4 (Fig. 3.7) there is the high tension supply, a variable transformer T10 and the magnetization current supply. T10 is the variable transformer for controlling the output power. A smoothing circuit (CH6, C22 and C23) is also incorporated in the high tension supply unit (T6, V8, V9). The transformer T8 and SR2 the bridge rectifier consistute the magnetization current supply. There are also safety devices SW2 to the door at the rear of the generator which is operated by the contractor CR1, a lead to the cooling fan of the output valves V1 and V2 (Chassis 1), and the input socket to the generator. Chassis 3 contains control circuits for the magnetization current supply to the three

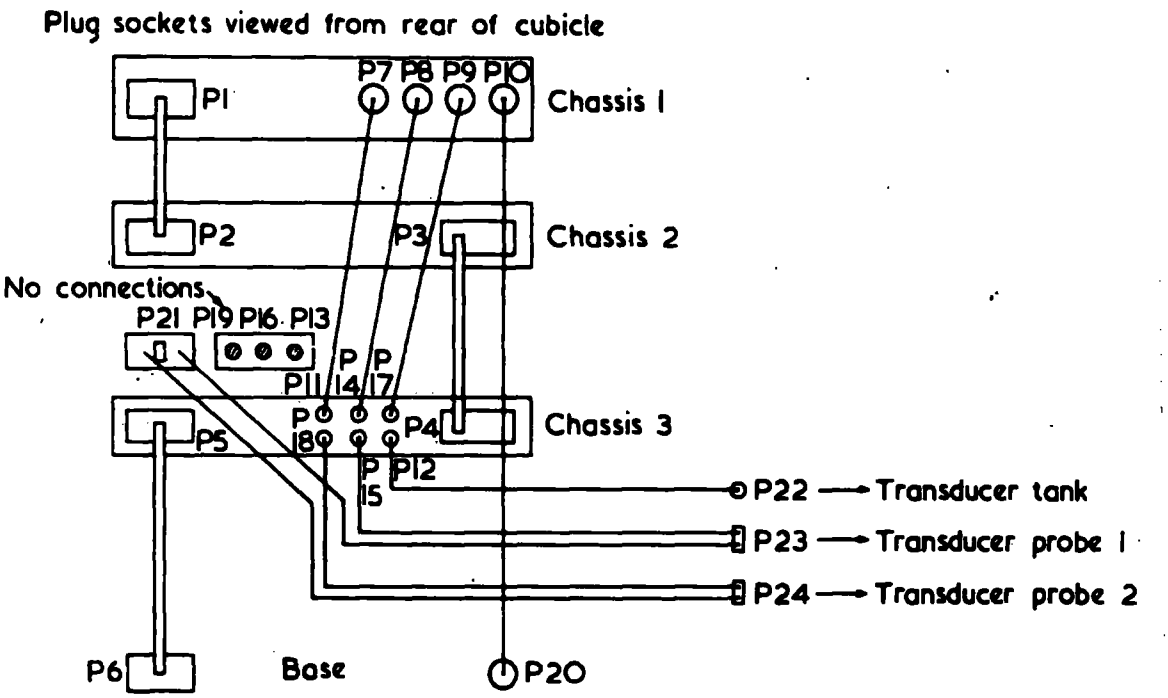

Fig.3.5. Block diagram of the electronic generator.

Fig.3.6a. Front view of the 2.0kW generator for driving magnetostrictive transducer unit.

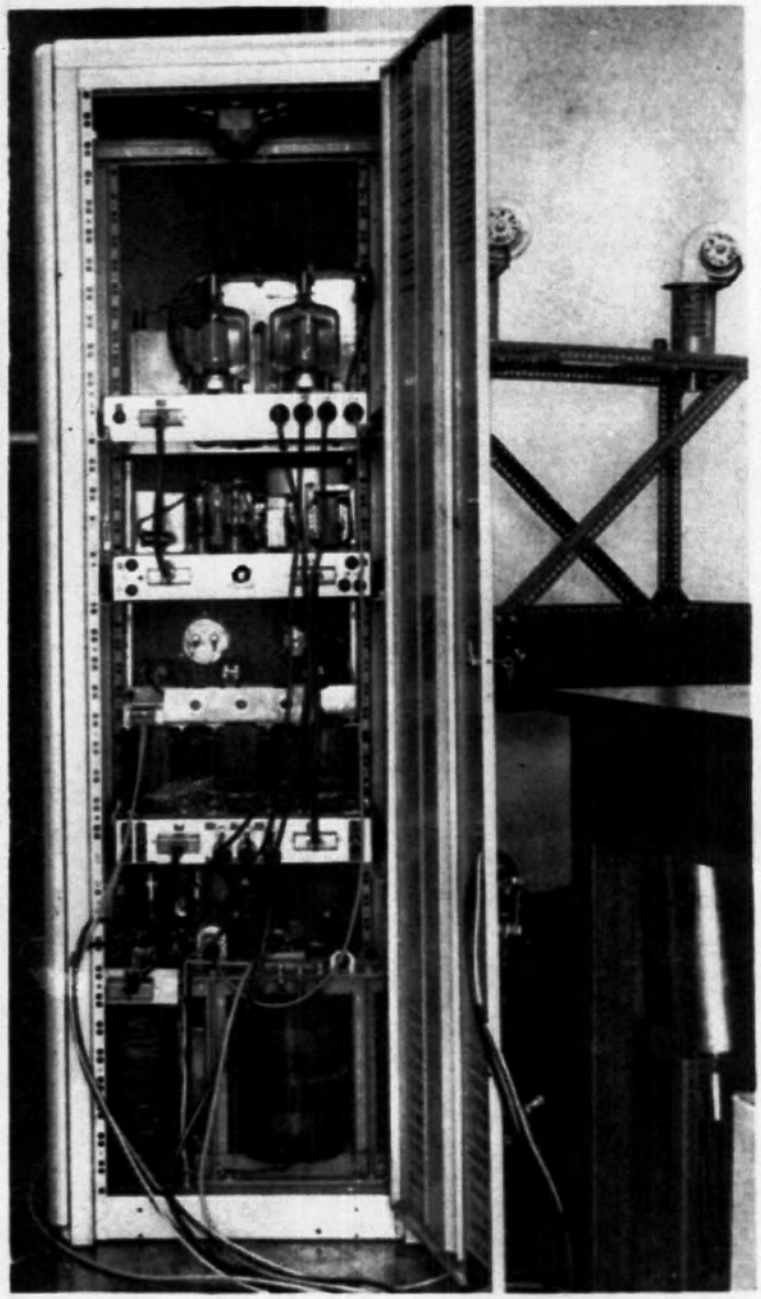

Fig.3.6b. Rear view of the 2.0kW generator for driving magnetostrictive trancducer unit.

sets of transducers. Included in this unit are four adjustment knobs; one for the choice of probe in seperate operations and three (VR2, VR3, VR4), for varying the magnetization current which can be read on the meter provided (Fig. 3.6a). There are also in chassis 3 a choke rejector (CH3, CH4, CH5) for each transducer unit and the blowing fan circuit for cooling the transducers. The choke rejector offers a high impedance to the oscillatory current and a low resistance to the d.c. polarising current thereby separating the two currents at the input to the transducers. Tappings (P13, P16, P19) to dummy loads are also provided for all three units. Dummy loads are used to maintain a fixed input power when it is necessary to switch off anyone of the three units in the case of simultaneous runs of the transducers.

Chassis 2 can be divided into four units (Fig. 3.7)

(1) the rectifier (T3, V3) and the smoothing unit (CH1, C7, C8, R17), which supplies a D.C. voltage (600V) to the screen grid of the output amplifiers (V1, V2 - Chassis 1).

(2) the rectifier (V4) and the smoothing unit (CH2, C9, C10) providing a 300V d.c. to the oscillator (V6) and the driver unit(V7).

(3) The oscillator unit with a 180° phase shift network (C15 to C18 and R8 to R12).

(4) The driver unit to which may be added the transformer T9 and the rectifier circuit (SR1, R19, C21) which supplied the grid bias of V1 and V2 (Chassis 1). T9 is a phase splitter for the output amplifiers. A thermo-delay unit is also built into chassis 2. It has a delay time of 30 secs. during which time the output amplifiers do not function. The mains indicator lamp is also in this chassis. Chassis 1 contains the output amplifier, the output transformer, T2; the D.C. blocking condensers, (C_1, C_2, C_3); and the circuit for the high frequency current meters and indicator lamps. The output amplifier is a push-pull amplifier (V_1, V_2) and separates the

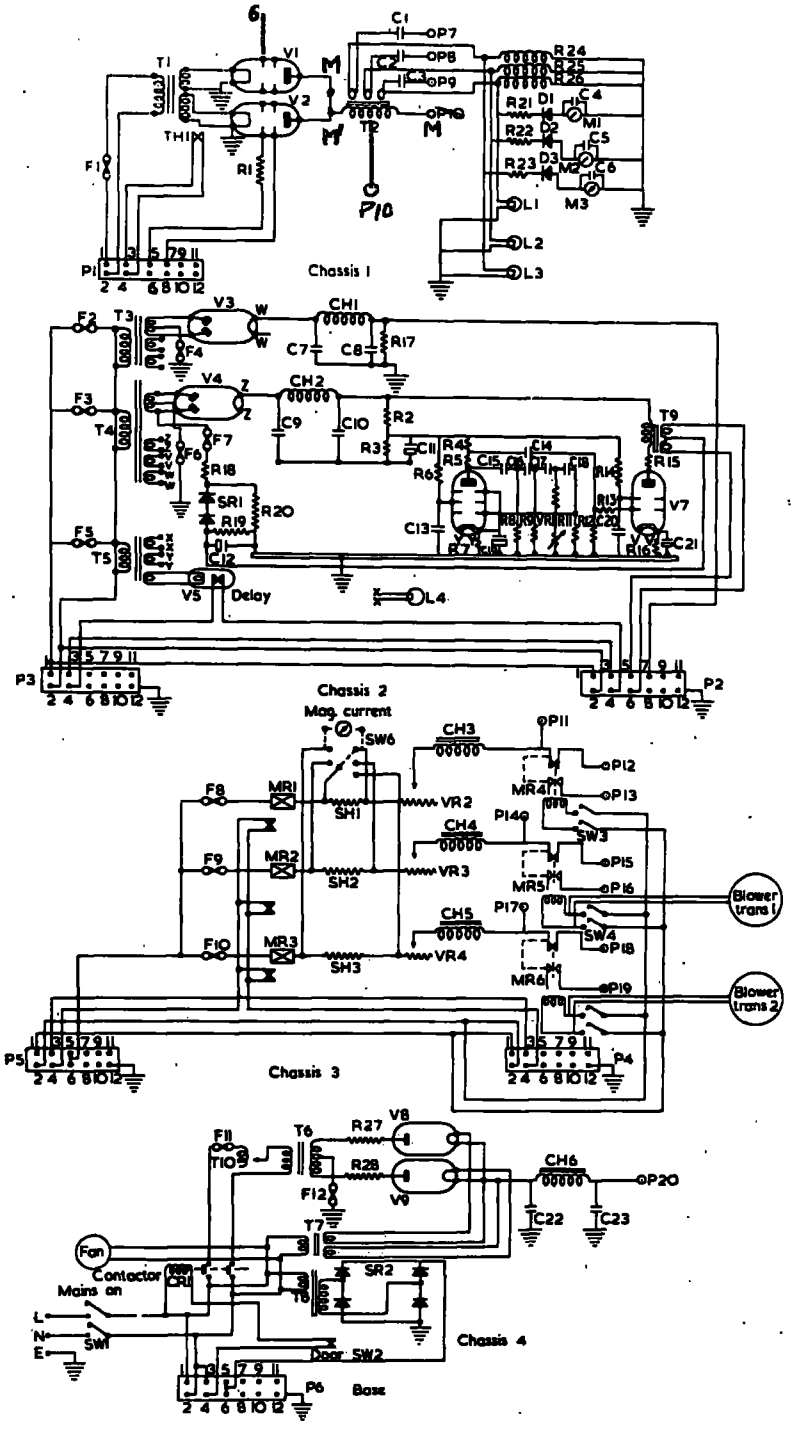

Fig.3.7. Circuit diagram of the 2.0kW generator. The chassis are numbered from top to bottom.

oscillator (chassis 2) from the transducer. Alterations to this part of the circuit, made after preliminary experiments, are shown in red (Fig. 3.7) on the circuit diagram. The tapping 6 of point P1 is now connected to the grid of valve V1 and P10 is now connected to the grid of valve V1 and P10 is replaced by a central tapping of the transformer, T2; while the points M are joined together. MM' does not exist any longer. The blocking condensers (C_1, C_2, C_3) perform the same job as the choke-capacitance coupling, CH3, etc. (Chassis 3) but this time, C_1, C_2 and C_3 block the d.c. current by presenting a high resistance.

Operation of the unit requires the closing of the switch SW1 on chassis 4, adjustment of the variable transformer T10, and adjustment to the required magnetization current value by the use of VR1, VR2, or VR3, in chassis 3. For the operation of a single transducer unit, the unit is selected by the means of a knob (Tank, 1, 2) on chassis 3 and the corresponding switch (SW3, SW4, SW5), closed. After a time delay of 30 seconds, the increase high frequency control is operated, a lamp is illuminated and the relevant high frequency current meter can be read. The lamp, L4, illuminates when SW1 is closed and the end of the delay period is indicated by a click from the generator. The operational characteristics of the generator are shown in Fig. 3.8 for four values of magnetization current. Inside the generator, there is a control for the fine adjustment of frequency (Fig. 3.6b).

3.4 EXPERIMENTAL SET-UP

A magnetostrictive transducer unit was chosen in preference to a piezoelectric unit for the project because of :

1. The high Curie point which permits the use of magnetostrictive transducers at the necessary high temperatures.
2. It can drive the high impedance load (water) into which it worked.

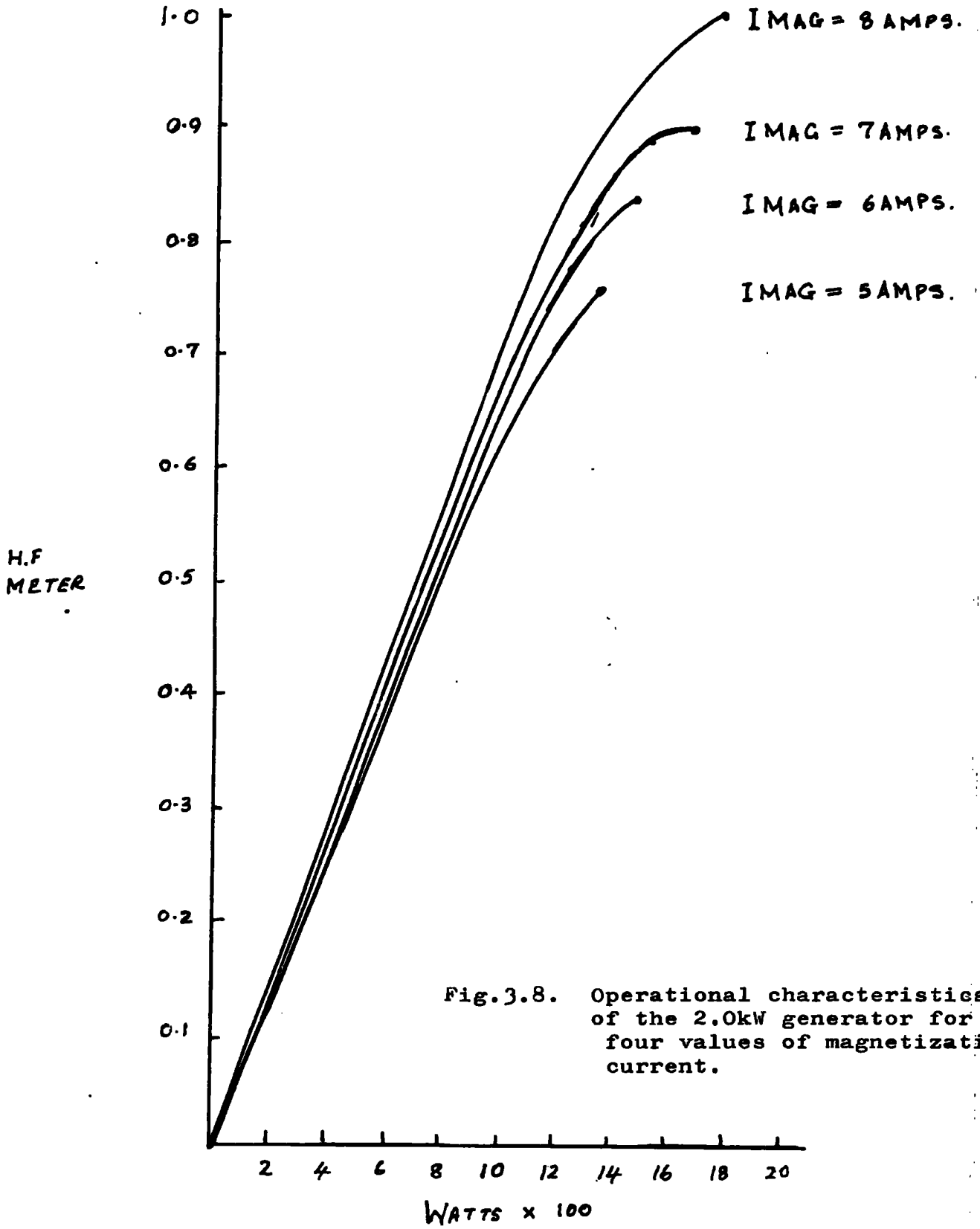

Fig.3.8. Operational characteristics of the 2.0kW generator for four values of magnetization current.

3. The coupling to the tank although critical is simple.

Apart from the electronic generator the complete equipment includes a constant temperature bath or tank and a transducer unit of a 3 in diameter stainless steel piston to which are attached four laminated rod transducers. The transducers constructed of 4% Co-Ni are of length 4.5 in so as to resonate at 20 kc/s and they have a Curie point of 410°C. Coils for the production of magnetic field are wound on four non-conducting cylindrical materials into which the transducers can easily be pushed. A metal cage protecting the transducers and coils has an electric motor and a fan (Fig. 3.7 - Blower) mounted at its lower end. Fig. 3.9 is an illustration of a complete transducer unit.

A typical transducer-tank coupling system is shown in Fig. 3.10. The magnetostrictive transducer is normally coupled at a nodal point i.e. the bottom of the tank is a node. It will be seen that the ends of the nickel rods and consequently the ends of the stainless steel piston are at antinodes. As mentioned above, a constant temperature tank (or bath) was used in the project. It is constructed of stainless steel with an outside casing of plywood and has internal dimensions 61 cm x 30 cm x 28.5 cm. The thickness of the plywood is about 1.7 c.m. A tap is fitted at one end of the bottom of the tank so that water can be run out at the end of a day's run. Transducer-tank coupling is very critical and requires that the bottom of the tank must be very flat. Coupling was effected by the use of eight 3/16" screws with plastic washers and a 0.2 cm thick rubber plate (i.d. 3", e.d. 3.5") in between the piston flange (Fig. 3.9) and the bottom of the tank. Both the rubber plate and the piston flange rest on the bottom of the tank. The best condition for operation is when the screws are just tight enough to prevent the dripping of water and the piston

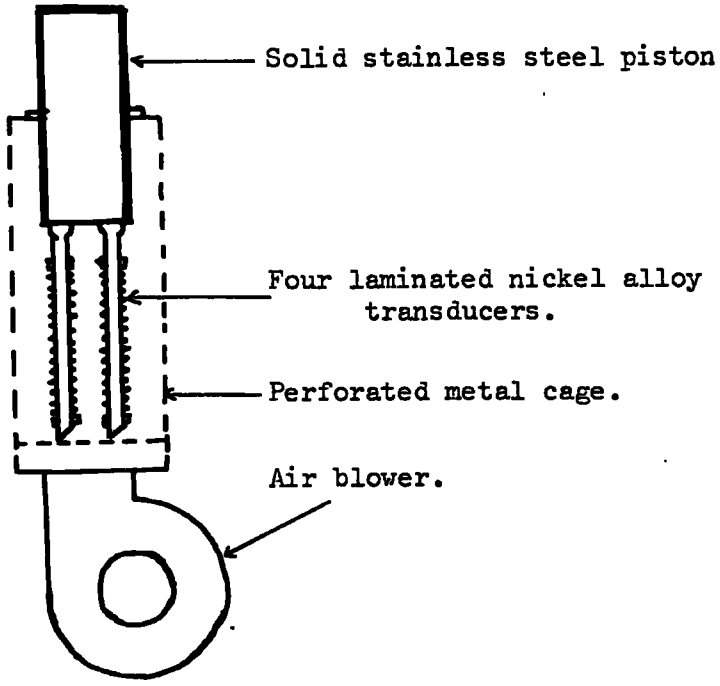

Fig. 3.9

Flange mounted probe surrounded by metal cage and cooled by air blower.

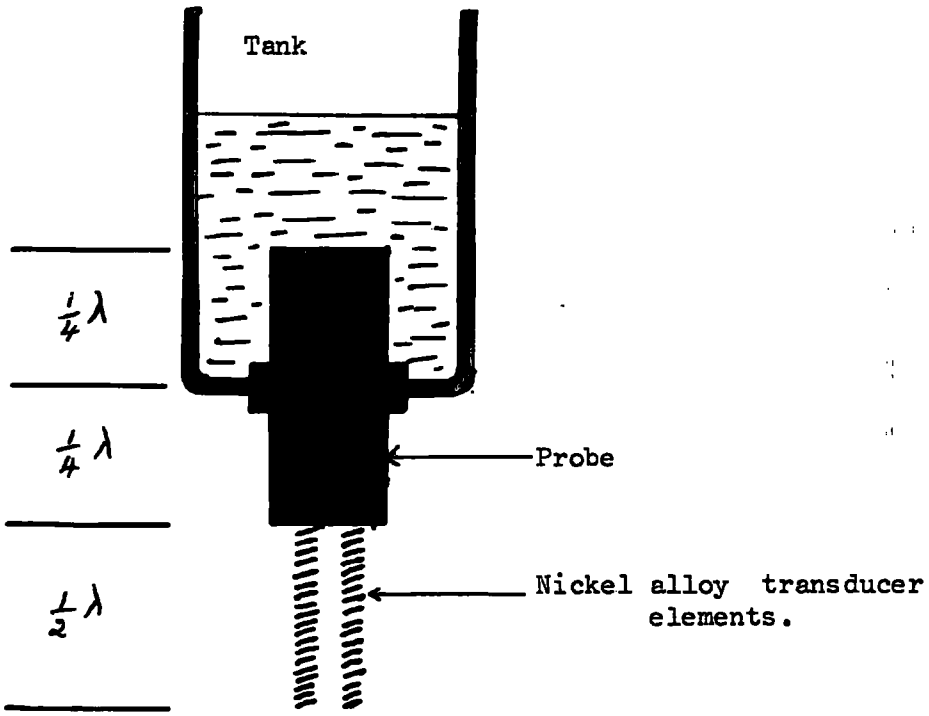

Fig. 3.10

Typical magnetostrictive transducer unit coupling system.

is still free to vibrate on its own. For a working height of 16.5 cm above the piston face, the tank takes about 45 litres of de-ionised water and using 14.55×10^{2} m/s as the velocity of ultrasonic waves in water, at 20 kc/s, the wavelength for standing waves is given by

$$\text{velocity} = \text{frequency} \times \text{wavelength}$$

as $7.275 \approx 7.28$ cm.

The metal cage protecting the transducers and coils is screwed at four points to strips of stainless steel soldered to the under-sides of the bottom of the tank. This coupling also affects the vibration of the transducers and must not be too tightly screwed in. For both couplings of the transducers and metal cage, cavitation noise provides an easy check since a maximum cavitation noise is obtained only at the best conditions for operation.

The suspension device for test samples is illustrated in Fig. 3.11. A is a brass plate 30 cm x 9.5 cm supported by four brass tubes 10.5 cm long, the brass tubes being soldered to two equal lengths of brass angles of length 50 cm (L). The solid brass rod, B, has a 2.54 cm. long tapping at its lower end, the rest of it is counter bored and the lower end is soldered to the plate C. The moving unit M, N and D are supported by the studded rod G which runs through B and is screwed below D. M is an optical lens holder system in the horizontal plane with the two rods N screwed into it; and provides a firm grip for glass test tubes. Lead samples are suspended from D which is soldered to the rods N. The height traversed by the moving unit can be read from any of two scales on the rods N with the top surface of A as reference. Support for the entire system is achieved at one end of the brass angles, L, by clamping to a rigid table. Both

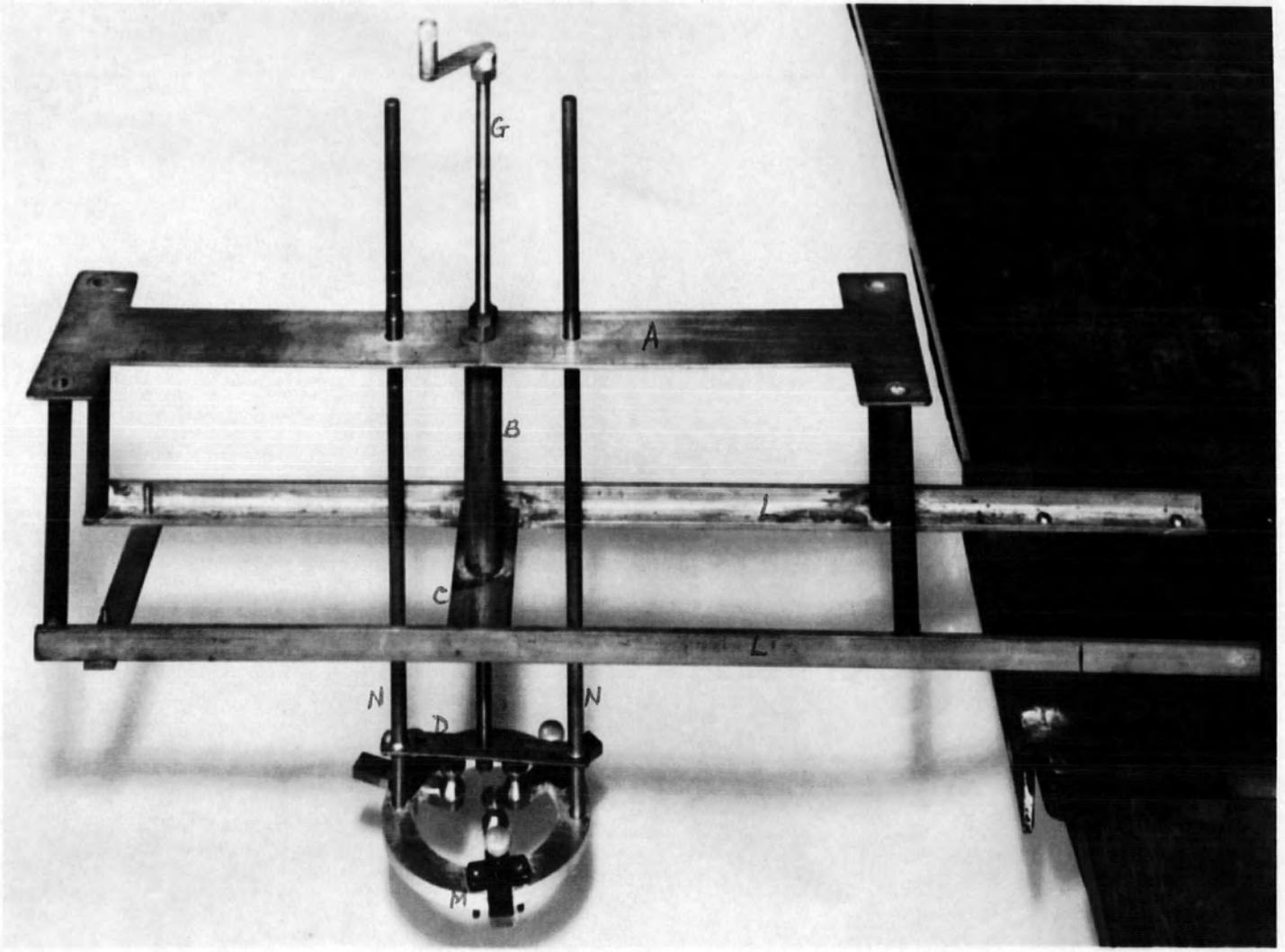

Fig. 3.11

Suspension Device used in cavitation activity measurements.

the table and the system are free of the constant temperature tank and are not effected by the vibrations of the transducers. There are no horizontal motions and the system is set with M vertically above the stainless steel piston of the transducer. The set up of tank and suspension device is shown in Fig. 3.12. A mercury-in-glass thermometer for readings of the temperature of the water in the tank can be seen at the end of the tank opposite to the thermostatic control unit.

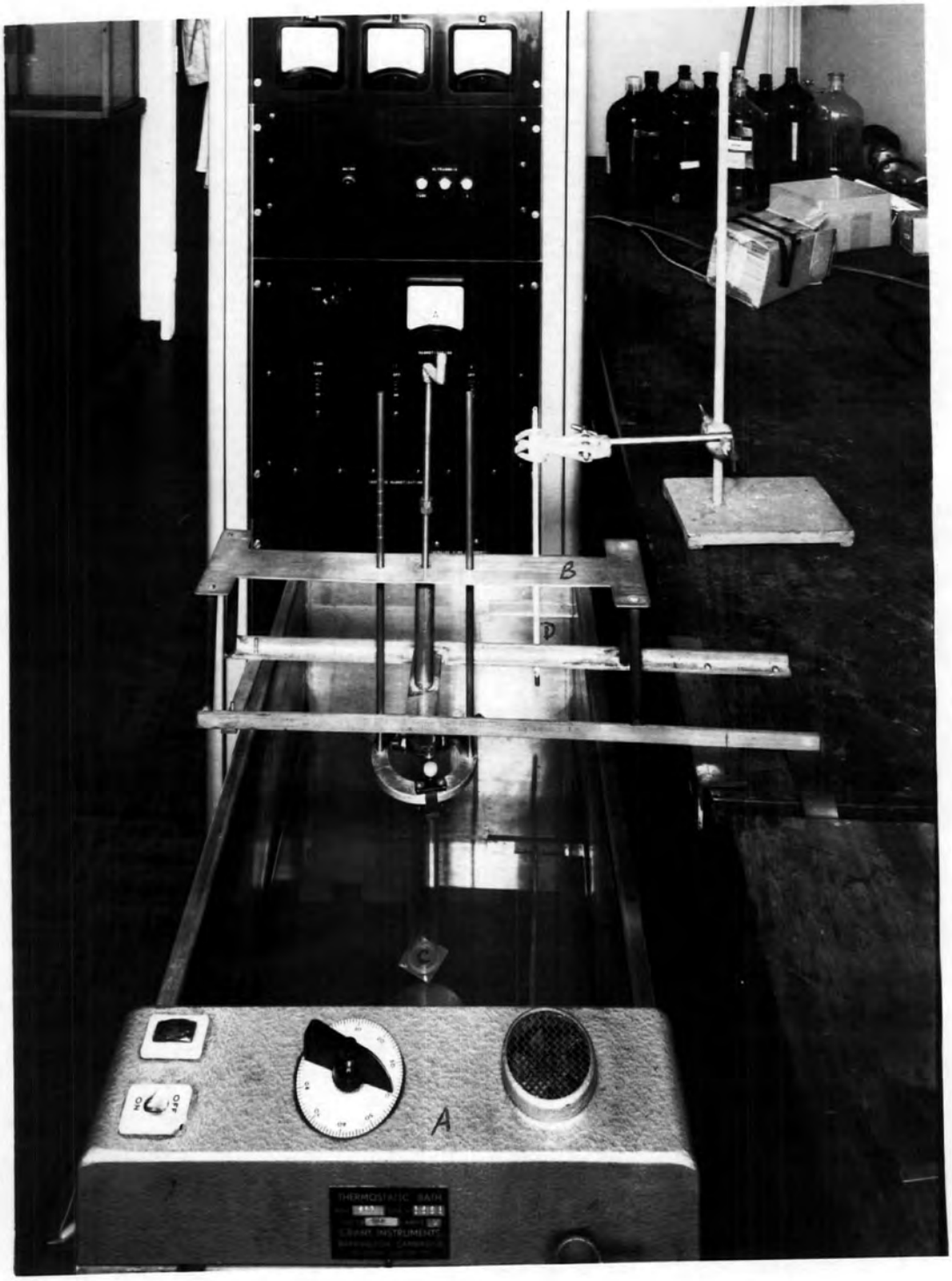

Fig.3.12. Experimental set-up. A. Constant temperature tank, B. Suspension device, C. Test tube, D. Mercury-in-glass thermometer.
The generator is at the background.

CHAPTER 4.

Several applications of ultrasonics are in liquid media and under suitable conditions cavitation may be produced in the liquid. The destructive nature of cavitation makes it essential that one should know the intensity of cavitation suitable for a specific application. [4.1] In Chapter 2, the two most commonly employed methods for the determination of the intensity of cavitation were enumerated. The first is based on the yield of free radicals from a chemical solution - Chemical Method [4.2] - and these effects are thought to be related to the gas-phase of cavitation bubbles. [4.3] Depending on the chemicals used, the relative intensity of cavitation may be expressed in terms of optical density, or grams of iodine, chlorine, etc. liberated. [4.4] The second, a primary effect of cavitation occuring in the liquid phase is cavitation erosion and cavitation ability is assessed by the loss in weight of a sample. [4.5]

4.1 PREVIOUS EXPERIMENTAL RESULTS AND OBSERVATIONS.

EROSION METHOD :

In 1960, L.D. Rosenberg investigated the mechanism of ultrasonic cleaning by the erosion method. He used aluminium, lead, gold, ceramics, plastics, etc. as his test samples in different liquids which show no chemical activity in respect to an experimental material. He worked at a frequency of 8 kc/s and expressed the magnitude of erosion and hence cavitation cleaning ability as the loss in weight (Δm) from a standard specimen weighed before and after irradiation. Rosenberg established that except for an initial period of 5 minutes, the erosion is directly proportional to the irradiation time and that during the first 5 minutes, the process is not so fast (for lead, aluminium and gold). Most important of all, he investigated the dependence of the relative intensity of

cavitation upon temperature for a range of -10° to +90°C. Using aluminium as the test sample in water, he observed an increase in Δ m with increasing temperature to a peak at 50°C, followed by a decrease in Δm for further increases in temperature. (Fig. 4.1). Moreover, he reported that the position of the maximum and also its absolute value depended essentially upon the liquid investigated; the absolute magnitude being greater in water than in other liquids.

CHEMICAL METHOD :

The chemical method of assessing the relative intensity of cavitation was investigated by A. Weissler. He used a solution of carbon tetrachloride in water with ortho-tolidine reagent as the indicator of the free chlorine. The intensity of the resulting yellow solution was measured in a Beckman spectrophotometer for blue light of 436 mμ wavelength and recorded as the optical density. (D_{436}). Working at a frequency of 28 kc/s and for an irradiation period of 10 seconds, he investigated the error that might arise from the concentration of ortho-tolidine reagent and also the irradiation time dependence of the intensity of the yellow solution. He observed that above 0.2 ml of reagent in 20 ml of carbon tetrachloride solution, the colour intensity was not affected by the amount of reagent and also that the intensity of the yellow solution increased linearly with time of irradiation. Like Rosenberg, Weissler observed the variation of the intensity of cavitation with temperature. A steady decrease in optical density with increasing temperature over a range of 10° to 70°C was reported.

An interesting proposition [4.4] was to express ultrasonic cleaning ability in terms of cavitation as

$$\sum_i a_i \, n_i \qquad 4.1$$

where each i represents a characteristic class of cavitation events (gassy or vaporous; steady-state or transient); each n is the number

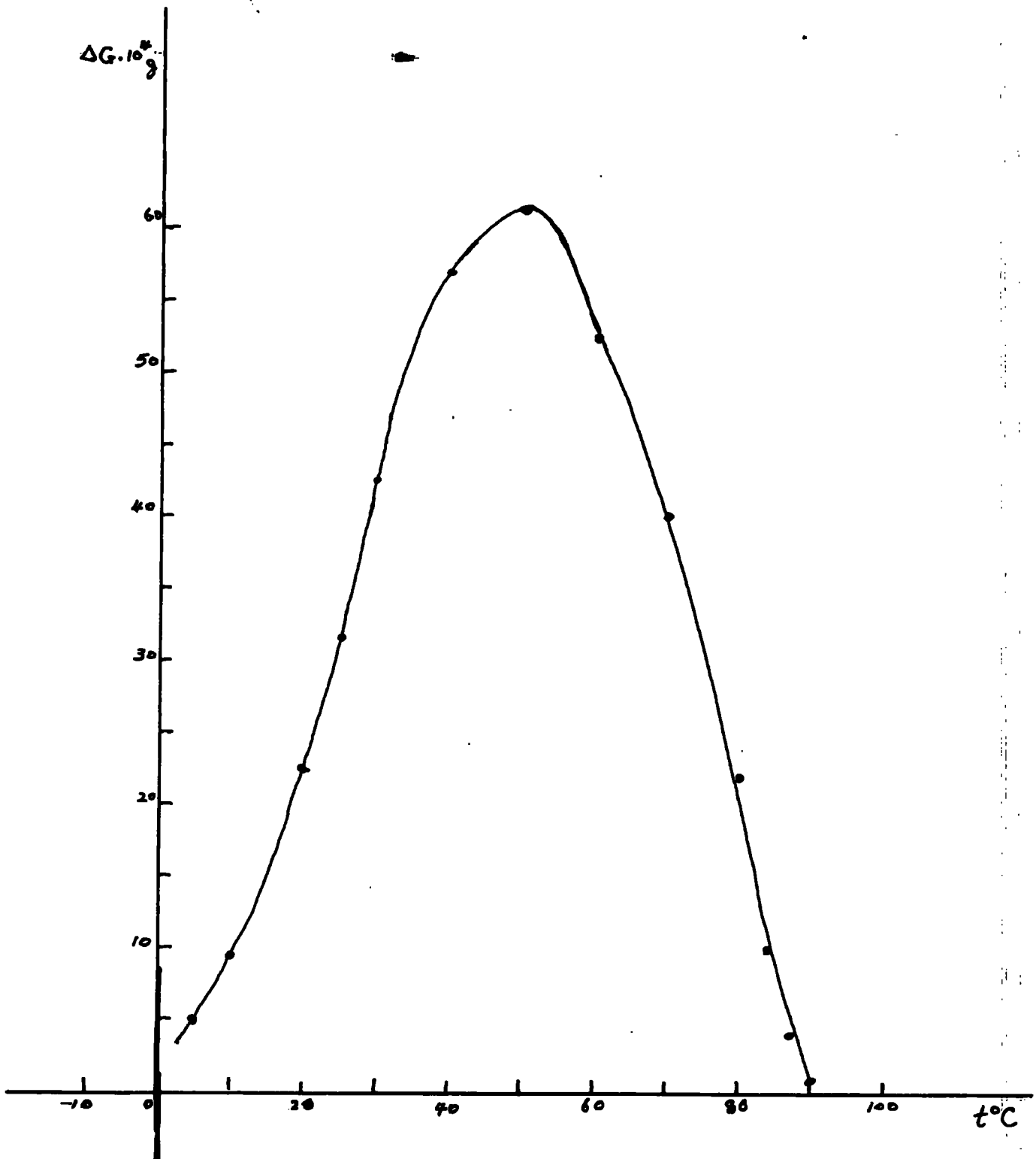

Fig.4.1 Cavitation erosion as a function of temperature for aluminium in water.

of events of this class per second, per unit volume, under the specific set of conditions; and each a is a co-efficient which expresses the relative cleaning effectiveness for this class of cavitation. The n's will be functions of such factors as temperature, frequency, dissolved gas content, treatment time, etc. The double integral of $\sum_i a_i n_i$ over the time of treatment and over the specific volume within the cleaner tank; it was suggested, maybe a more elegant expression.

Weissler also suggested that the quantitative ability of ultrasonic cavitation to promote chemical reactions could be represented by a similar expression,

$$\sum_i b_i \, n_i \qquad 4.2$$

where each b is the co-efficient of relative sonochemical effectiveness for each class of cavitation; and that the ratio a_i/b_i could be assumed more or less constant at least for a particular ultrasonic cleaner at a particular frequency.

The third section of the proposition suggests a simple relationship between a_i and b_i and consequently, between cavitation erosion and cavitation promoted chemical reactions. On the other hand, experimental observations of the relative intensity of cavitation with temperature by both erosion and chemical methods given above, suggest that the relationship between a_i and b_i may not be a simple one.

4.2 EXPERIMENTAL PROCEDURE.

Two important features of the last section are :

(a) the differences of the observed results for the variation of the relative intensity of cavitation with temperature, and

(b) the propositions of Weissler.

The first suggests the need for some work by both erosion and chemical methods under identical conditions of frequency,

power input to the same transducer, height of test samples above the transducer face, etc. The second suggests the need for two mathematical expressions for the results obtained for both methods and an investigation into the possibilities of finding a relationship between the two expressions, leading to the ratio a_i/b_i. These factors determined the choice of the complete equipment and experimental set-up described in the last chapter.

CHLORINE LIBERATION METHOD :

Preparation of Solutions :

Two solutions were needed. The first was a concentrated solution of carbon tetrachloride in water. 4 ml of carbon tetrachloride to a liter of deionized water was vigorously shakened up in a brown bottle and allowed to settle overnight. The process of shaking was continued the following day until the carbon tetrachloride was broken up into small pellets whose adhesive forces were small enough to avoid possible coalesce. At this stage, a fine suspension of carbon tetrachloride in water had been obtained and the solution was considered ripe for use after settling overnight. The second solution was 0.675 gms of ortho-tolidine reagent dissolved in a mixture of 75 ml of concentrated hydrochloric acid and 425 ml of distilled water. Like the first solution, this was stored in a brown bottle to minimize deterioration. Weissler used 2 ml of carbon tetrachloride to the liter of distilled water but the ortho-tolidine reagent solution was of the same proportion as above.

Test cells used for irradiation were made of glass tubes 10 cm. long and 2.54 cm. internal diameter to the bottom of which were cemented 3 cm square polythene sheets of thickness 0.5 mm. Polythene was used for the sake of greater transparancy to ultrasonic waves. The cementing was with araldite and the cells were left

overnight for the araldite to harden. This procedure was repeated before an exposure and the glass tubes were cleaned by ultrasonic waves. The cleaning of the test tubes and in particular of the brown bottles for storing the solutions was very essential as it was observed that the presence of dust particles or dirt resulted in the separation of carbon tetrachloride from the suspension or solution.

Procedure :

Twenty ml. of carbon tetrachloride solution and 1 ml. of ortho-tolidine reagent were pipetted into a test cell and the cell clamped in place, vertically above the transducer piston by the use of the optical-lens-holder system M (Fig. 3.11). The height of deionized water in the tank was 16.5 cm. over the transducer face and the bottom of the test cell 3.5 cm. above the transducer face. Unlike the method employed by Weissler, the liquid level inside and outside the tube were not the same; the height inside the tube being lower than that outside the tube. The height of 3.5 cm. above the transducer face was chosen so as to avoid working at a nodal point of the standing waves that were set up in the water; and also to avoid the loss of energy due to attunation by dispersion and absorption.

Before the test cell was clamped into position, the water in the tank was degassed for a total period of 30 minutes. The process was conducted in two stages of 15 minutes each, with a 10 minutes interval for the generator to cool down. For all the irradiations, a period of 3 minutes at least was allowed after the test cell had been clamped into position for thermal equilibrium. Ultrasonic irradiation time for each run was 120 ± 0.1 seconds. A complete absorption spectrum of the resulting yellow colour was plotted using a UNICAM spectrophotometer (S.P. 700), in the visible region of light (30ν to 14.5ν where ν is the wave number).

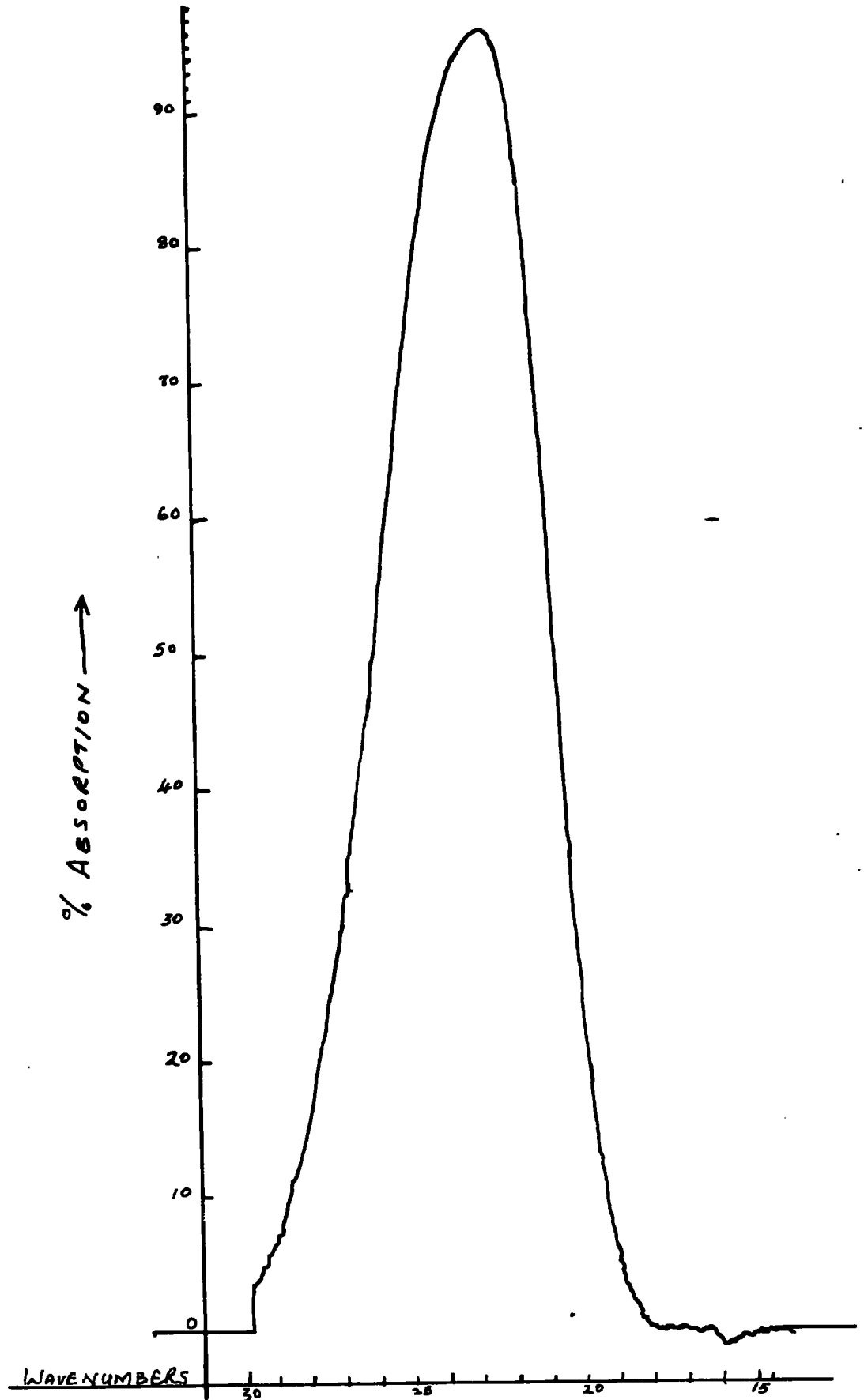

Fig.4.2. A typical absorption spectrum for yellow solution.

The plotting of the absorption spectrum required two solutions : the irradiated yellow solution and an unirradiated solution (20 ml. CCl_4 to 1 ml. O-tolidine reagent solution) termed the reference solution. Some of each solution was put in 1 cm. quartz cells - the sample cell and the reference cell- and clamped in the respective parts of the spectrophotometer. The operation of the spectrophotometer is automatic and it compares the percentage of light transmitted through the two solutions. Fig. 4.2 is an illustration of a typical absorption spectrum. The percentage transmission of light is given by

$$100 - A \qquad 4.3$$

where A is the peak percentage absorption. The peak at 22.8ν corresponds to 436 mμ wavelength and to the wavelength at which free chlorine gives a peak absorption spectrum. A total time of 15 minutes was spent on the entire process from pipetting the solutions into the test tubes to the completion of the plot of the spectrum.

The temperature range chosen was 20° to 80°C and values of optical density were determined at 21°, 28°, 36°, 45°, 55°, 65° and 75°C. Ten readings of optical density were obtained at each temperature reading except at 75°C where eight readings were taken.

OBSERVATIONS :

Standardization:

Standardization of the solutions and in particular the solution of carbon tetrachloride presented a problem. Carbon tetrachloride is inert and since only a little fraction of the 4 ml. used was dissolved, it was difficult to find a simple method of observing the concentration of the solution. The change in the density of distilled water was too small to be observed

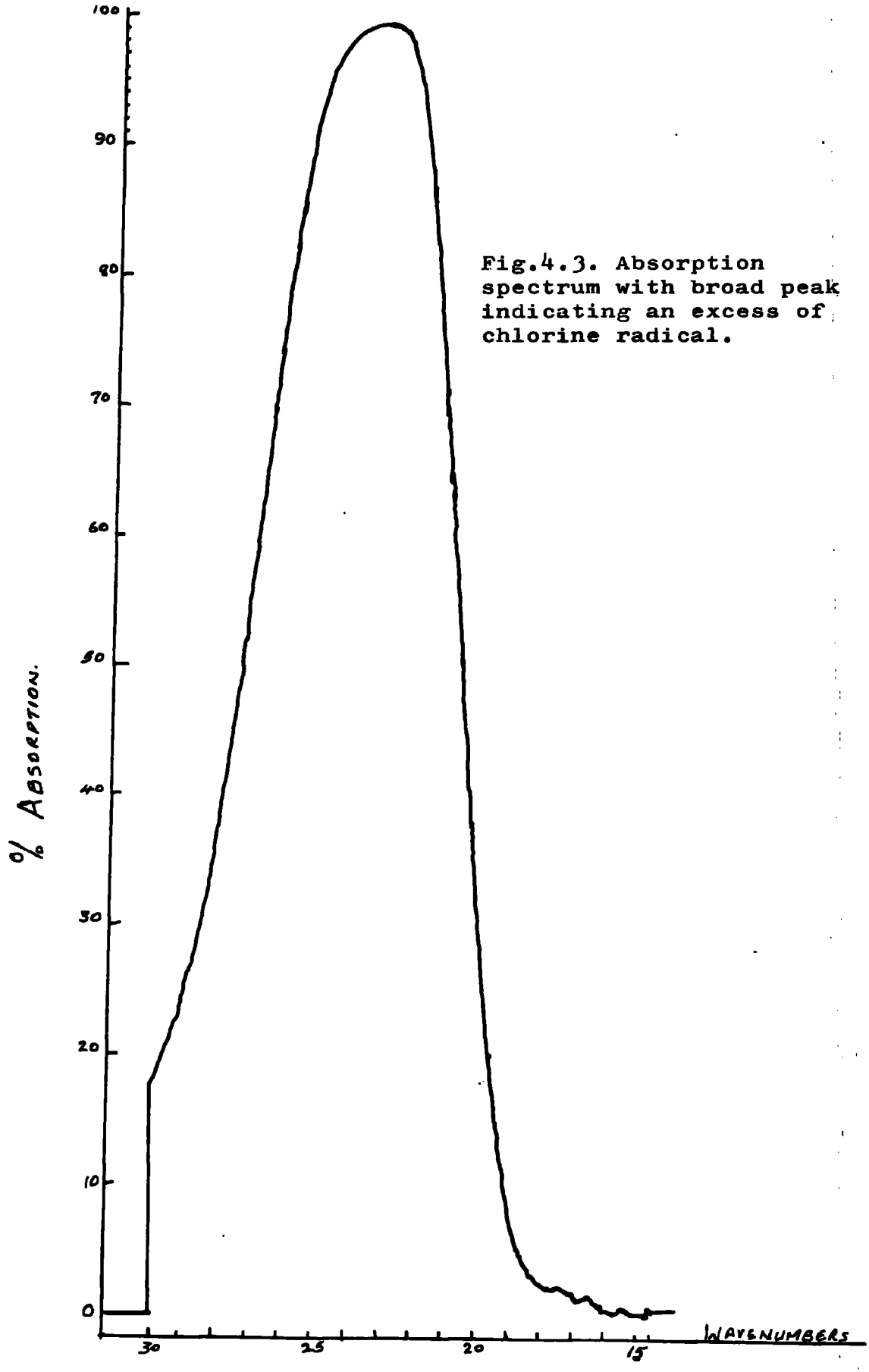

Fig.4.3. Absorption spectrum with broad peak indicating an excess of chlorine radical.

without too much error and as such, solutions were considered ripe if they gave the same percentage of transmission for blue light of 436mμ wavelength at room temperature (20°C). On the other hand, very highly concentrated solutions of carbon tetrachloride would give off more chlorine and a lower percentage of transmission. Such solutions could easily be detected since the absorption percentage for 120 seconds irradiation at 20°C was very near to 100; and excess chlorine liberation would result in broad undefined peaks. Fig. 4.3 is an illustration of such a spectrum.

Evaporation of Carbon Tetrachloride.

Preliminary experimental runs revealed that although optical density decreased with increasing temperature, there was a large drop in the readings at 50°C. Subsequent test runs at 50°C in which the thermal equilibrium period of 3 minutes was neglected showed some improvements in the results obtained. It was suspected that evaporation of the solution was taking place. This idea was based on the low boiling point of carbon tetrachloride and the fact that its evaporation would result in a lowering of the amount of free chlorine yield; and was confirmed as follows :

The water in the constant temperature tank was kept at room temperature (20°C), and two test tubes of solutions pipetted as above were used. One was irradiated directly at 20°C; the other was warmed to 50°C in a beaker of hot water, cooled to 20°C and then irradiated. The irradiation time in both cases was 120 seconds, and their spectra were plotted. Fig. 4.4 shows the absorption spectra for the two cases. The peak percentage absorption of the second solution at 436 mμ was much lower than that of the first due to evaporation losses. A repeat of this procedure was carried out, more ortho-tolidine solution (1 ml.) being added to the second test tube of solution just before irradiation. As there was no

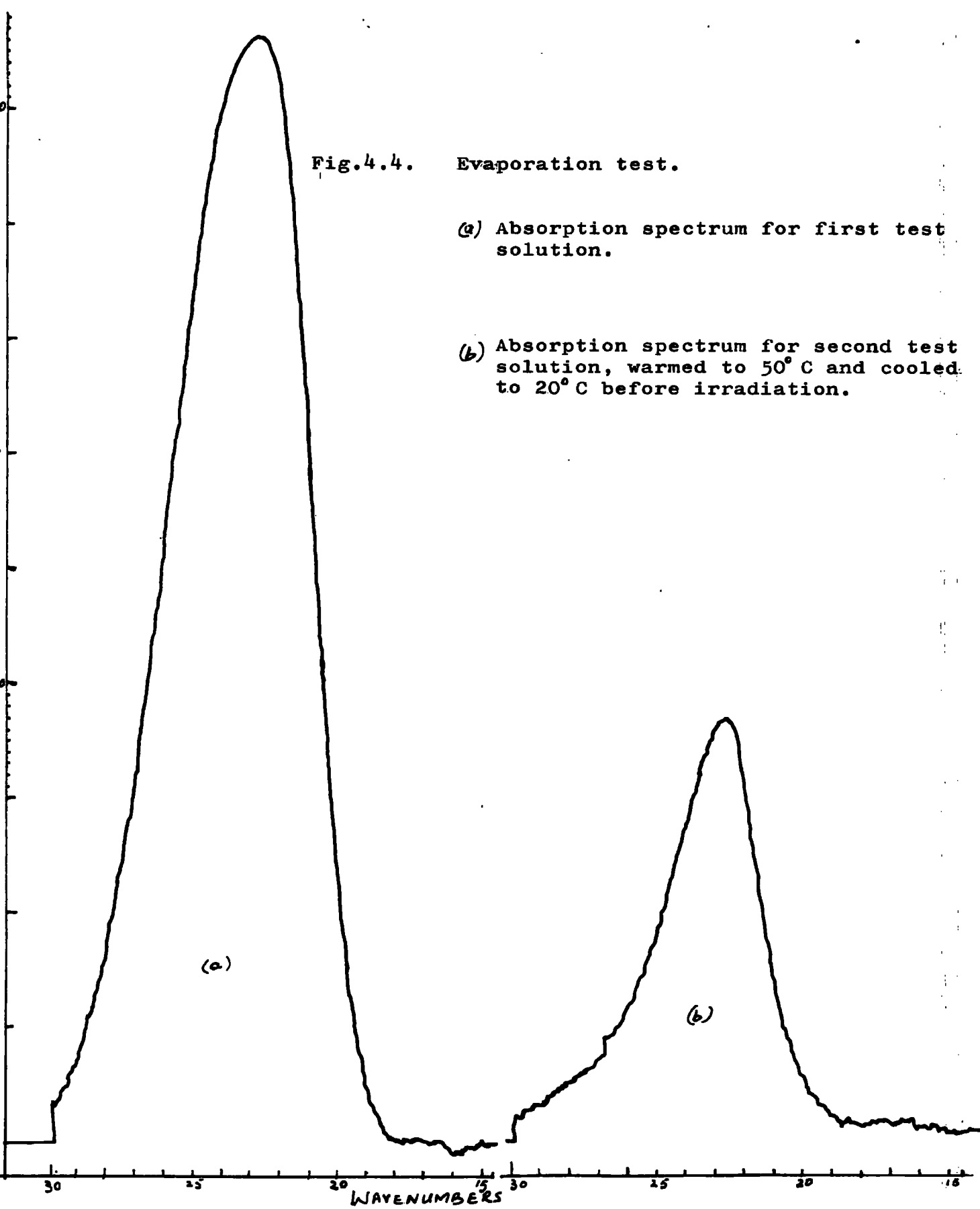

Fig.4.4. Evaporation test.

(a) Absorption spectrum for first test solution.

(b) Absorption spectrum for second test solution, warmed to 50° C and cooled to 20° C before irradiation.

improvement in the peak absorption percentage obtained, it was concluded that the carbon tetrachloride component was affected.

Similar tests were conducted for test solutions warmed to 30°, 40° and 80°C. Evaporation effects at 40°C were very slight; appreciable at 80°C and none at all at 30°C. Efforts to find a substitute solution that could withstand the above test failed; the following compounds and their combination having been tried:-

(a) $^{N}/_{10}$ potassium iodide solution to 1 ml of carbon tetrachloride with 1% starch solution as an indicator.

(b) 4 ml tetrachloroethylene to a liter of water and similar solutions of tetrachloroethane and benzotrichloride. The indicator was ortho-tolidine solution.

(c) $\frac{1}{100}$ Molecular weight of hexachloroethane dissolved in a liter of water.

(d) Combinations of tetrachloroethylene, hexachloroethane, tetrachloroethane and benzotrichloride in different proportions of water.

(e) The fact that ethylene glycol is soluble in water and that tetrachloroethylene, hexachloroethane, tetrachloroethane and benzotrichloride are all soluble in ethylene glycol was also tried out.

All tests gave yields of free chlorine with the usual yellow colour but none withstood the evaporation test. It was therefore decided to conduct the experimental work described above with carbon tetrachloride solution and in order to confirm Weissler's result, the temperature readings 20°, 28° and 36°C were chosen. Evaporation of carbon tetrachloride was later reported by Shih-Ping Liu [4.6] who used potassium iodide solution to which was added some carbon tetrachloride. Starch solution was the indicator and he observed that at and above 39°C (100°F), evaporation of carbon tetrachloride affected the results. This temperature reading is in agreement with the observed 40°C recorded above.

EROSION METHOD :

Preparation of Samples :

It was mentioned in Chapter 2 that the erosive effect of cavitation is reduced by the hardness of the material under attack. Most metals have an "incubation" period and as such, metal samples for the quantitative determination of cavitation must have little or no incubation periods. The sample must be of high density so that very little losses in weight can be accurately determined. Lead, aluminium and tin come within this group; but lead has the overall advantage of high density. The chosen metal must be easy to polish so that uniform finishing can be obtained.

Lead was chosen for the experimental work described below. A strip of chemically pure lead 100 cm x 6.5 cm x 0.65 cm thick was first rolled to a thickness of about 0.3 cm. Rolling was manual and might have effected the structure of the material. Thus, outstanding bumps were removed and the strip was cut into plates 5.2 cm x 5.2 cm x 0.3 cm thick, using a mechanically operated guillotine. A pressure machine loaded to 5 tons levelled out the plates, reducing their thickness to 0.25 cm. These plates should not be very thin as they could be torn to shreads when exposed to cavitation.

Five grades of emery cloth, Nos. 180, 220, 320, 400 and 600 respectively were used in the successive treatment of the surfaces and edges of the samples. In each case, the samples were polished in one direction by one piece of emery cloth and at right angles to this direction by the next piece of cloth. At this stage, all outstanding bumps and pittings had been removed from the samples, and they were finally treated with alumina for a uniform finish. Grades 5/20 - fast cutting, 5/30 - slow cutting and gamma - finish polishing alumina were used in that order.

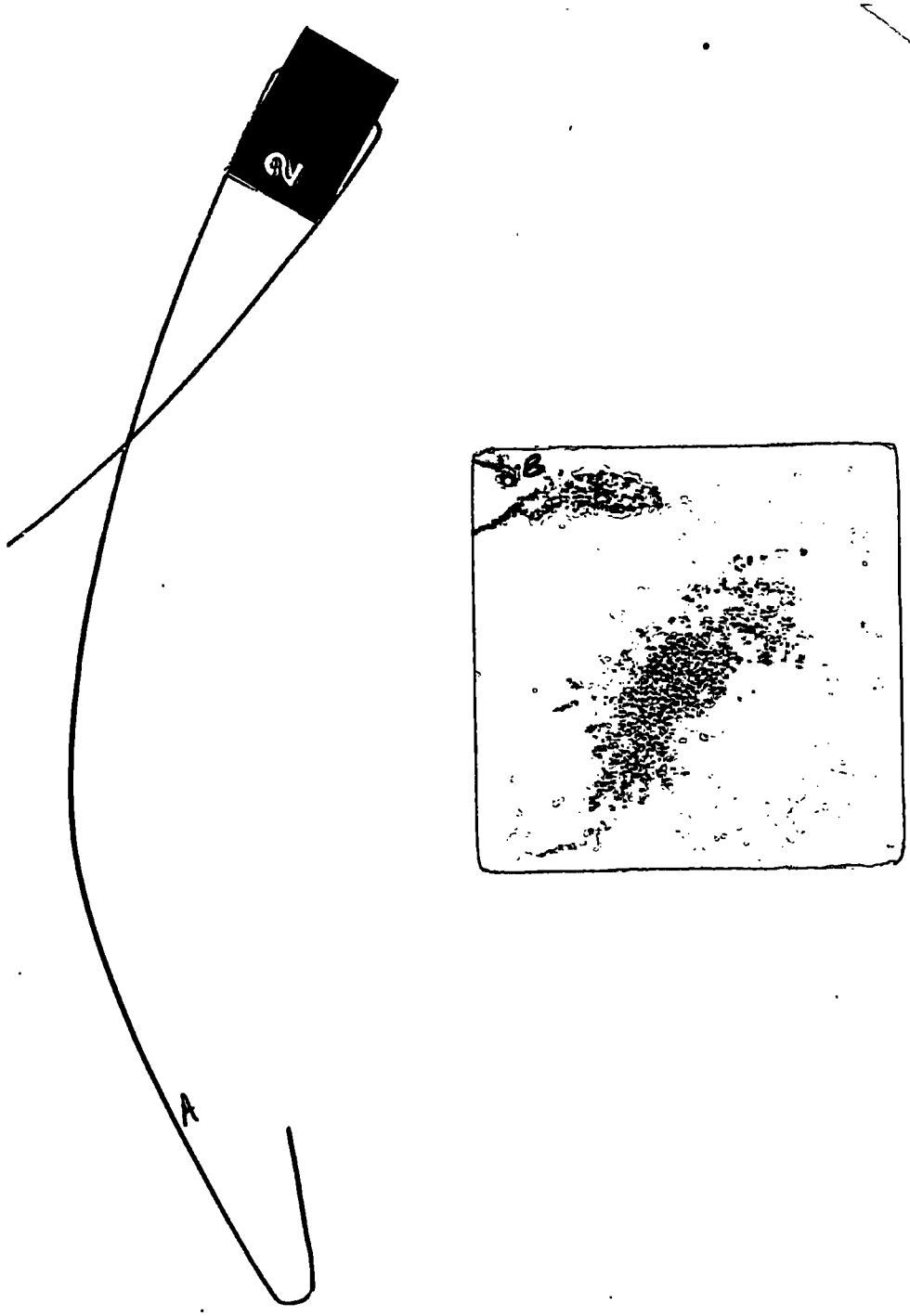

Fig.4.5. Erosion pattern on a lead sample after 40 minutes exposure to cavitation.
A is the metal wire threaded through the hole, B.

Procedure:

In each experiment, 1% of Teepol was added to the deionized water in the tank, to enable the water to thoroughly wet the samples. The water height of 16.5 cm over the transducer face was maintained and the manner of degassing the water was the same as in the chlorine liberation experiment. Two lead samples prepared as above were used at a time. They were washed in acetone, weighed accurately to four decimal places and then, suspended vertically in the tank of water by wires threaded through a hole drilled in one corner of each sample. The centres of the samples were 6.2 cm. from the transducer face and their lower corners at 3.5 cm. from the transducer coincided with the height of the bottom of the test tube used in the chemical experiment.

Irradiation of the samples in water medium lasted 40 minutes, their positions being interchanged after 20 minutes. At the end of the 40 minutes irradiation, the two samples were dried in acetone and carefully reweighed to determine the quantity of lead eroded. Experiments were carried out in this manner for a temperature range of 20° to 80°C at intervals of 21°, 30°, 40°, 50°, 60°, 70° and 80°C. Six samples were used at each temperature, working two at a time and a statistical average of the losses in weight determined. Fig. 4.5 shows a typical erosion pattern on a sample after 40 minutes exposure to cavitation.

GENERATOR : OBSERVATIONS.

Before all experimental runs described above were carried out, a frequency check on the generators was conducted (Fig. 4.6). The time calibration bright-up on the time base was obtained on the screen of the solarscope (Type CD. 643.2) for a frequency of 20 kc/s (i.e. time period = $^{1}/_{\text{frequency}} = 0.5 \times 10^{-4}$ sec). This was a straight line and when the high frequency current from the generator was switched on, a sine wave was imposed on the straight line. The magnetization current was 8.75 ± 0.05 amps and the high frequency variac was set at 210. By the use of the fine tuneing device in

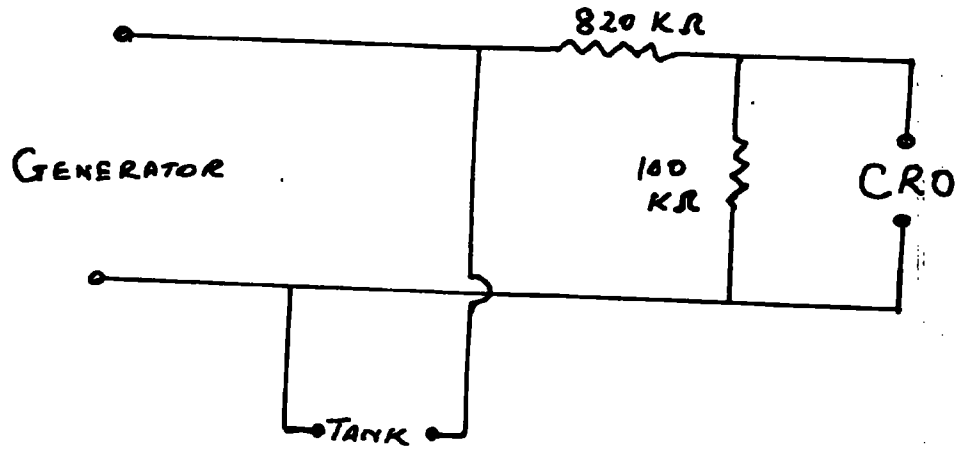

Fig.4.6. Circuit diagram used for frequency and power out-put check on the 2.0kW generator.

the back of the generator, maximum cavitation noise was obtained and the length of the sine wave was made to coincide with the length of the straight line. The solarscope gave a voltage reading of 430 volts, corresponding to 3956 volts across the transducer.

During the experimental runs, the magnetization current was kept constant at 8.75 $\pm$ 0.05 amps but the high frequency current varied. Below 50°C, the latter was observed to increase from 0.38 ma to 0.44 ma. for the chemical method and to 0.52 ma over the 20 minutes intervals of the erosion method. The variations above 50°C were much higher reaching 0.5 ma and 0.60 ma respectively. This had the effect of shifting the operational resonance frequency of the transducer especially in the erosion method where long periods of irradiation were necessary. The above effect was attributed to the alteration of the transducer impedance and loading with temperature. The mains input to the generator was not stabilized and it was observed that the generator was very sensitive to its fluctuations. Heavy loading of the mains or the sheding of the power supply to the locality usually resulted in very high and unstable values of high frequency currents.

CHAPTER 5.

5.1 RESULTS.

CHEMICAL METHOD:

The results obtained for the variation of the relative intensity of cavitation with temperature by the chlorine liberation method are given in Table 5.1 The figures given are the statistical averages of the readings at each temperature value and they are for ultrasonic irradiation periods of 120.0 $\pm$ 0.1 seconds. It can be seen that these results are in agreement with those of Weissler who observed a steady decrease in the optical density of the resulting yellow solution with rise in temperature. The errors quoted are the most probable errors and were derived from

$$\text{Error} = \pm \frac{0.6745\ \sigma}{\sqrt{n}} \qquad 5.1$$

where σ is the standard deviation and n is the number of values of optical density at each temperature value.

To facilitate comparison of the two methods used in assessing cavitation ability, the optical density per minute was determined and the results fed into a computer (KDF9) for the equation of the best fitting curve. In this case, all readings at each temperature value were used and the programming method is given in the Appendix. Fig. 5.1 is a plot of the best fitting curve derived by the computer. The other points which do not lie on the curve correspond to experimental results obtained at the respective temperatures. Using Weissler's suggestion, a polynomical was first plotted and its coefficients are in agreement with the equation of Fig. 5.1 i.e.

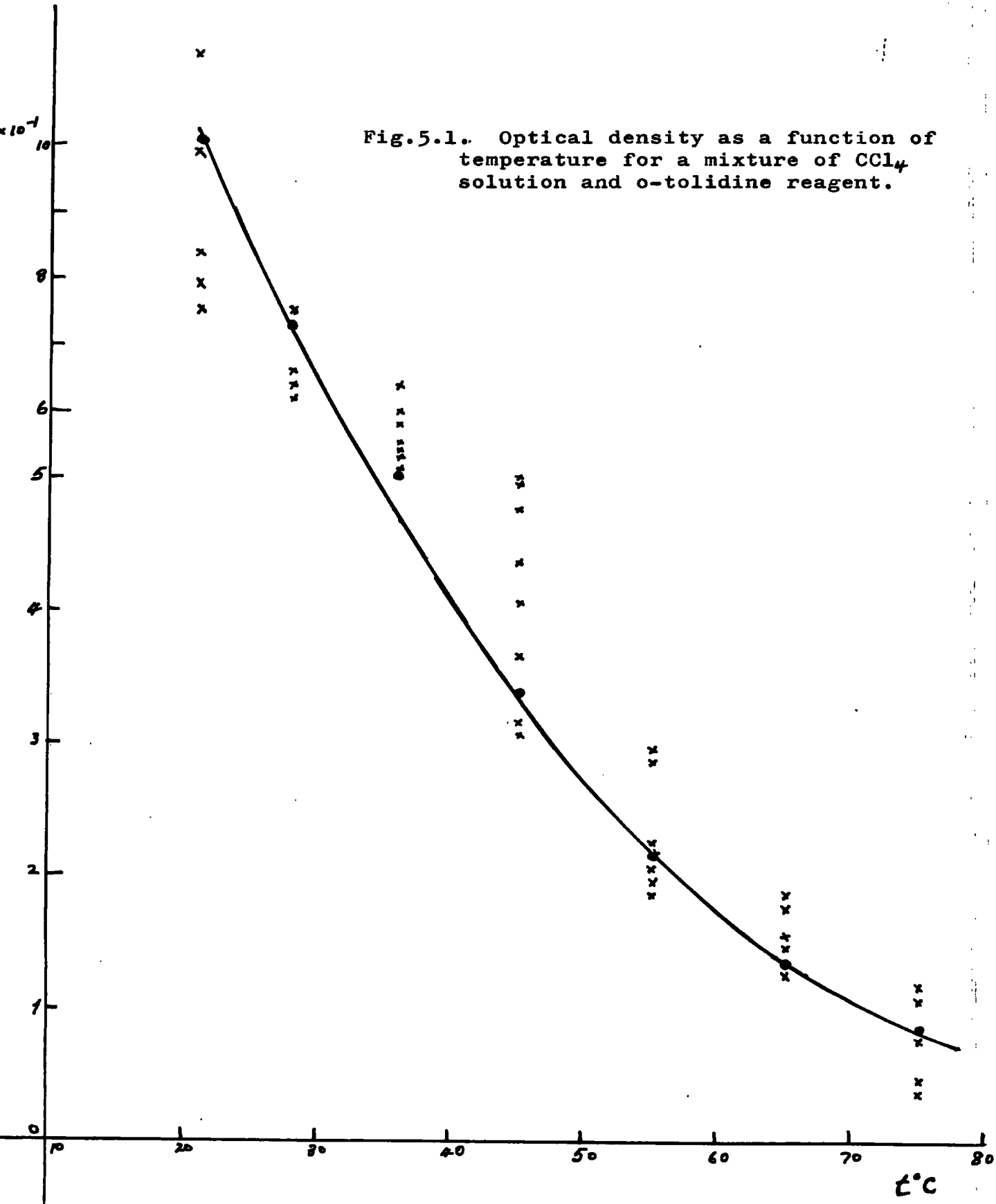

Fig.5.1. Optical density as a function of temperature for a mixture of CCl_4 solution and o-tolidine reagent.

$$D = 2.627 \exp. (- 0.045\ T) \qquad 5.2$$

where D is the value of optical density per minute at a temperature $T^{o}C$.

It should be observed that equation 5.4 does not account for the effects of evaporation of carbon tetrachloride on the values of optical density at temperatures above $40^{o}C$. Consequently, only the first three values in Table 5.1 are reliable. A modification to Eqn. 5.4 should include a factor, f(T), introduced to account for evaporation effects. f(T) will account for terms as, $(^{dm}/dT)$, the temperature rate of loss of carbon tetrachloride; $(^{dm}/dt)$, the time rate of loss and a transformation factor to convert these terms into units of optical density.

EROSION METHOD:

Fig. 5.2 is the graphical representation of the results obtained by the lead erosion method. The curve represents the best fitting curve calculated by the computer and the experimental results are also shown at each temperature reading. As in the chlorine liberation results, all experimental values were used in the computer data after the loss in weight per minute had been determined. The statistical averages of these results for 40 minutes irradiation are shown in Table 5.2 and the errors quoted were calculated using equation 5.1. The equation of the best fitting curve is

$$\Delta m = 1.534 \times 10^{-2} \exp. - \left(\frac{T - 52.5}{22.36}\right)^{2} \qquad 5.3$$

where Δm is the loss in weight (in gms/min) at any temperature $T^{o}C$.

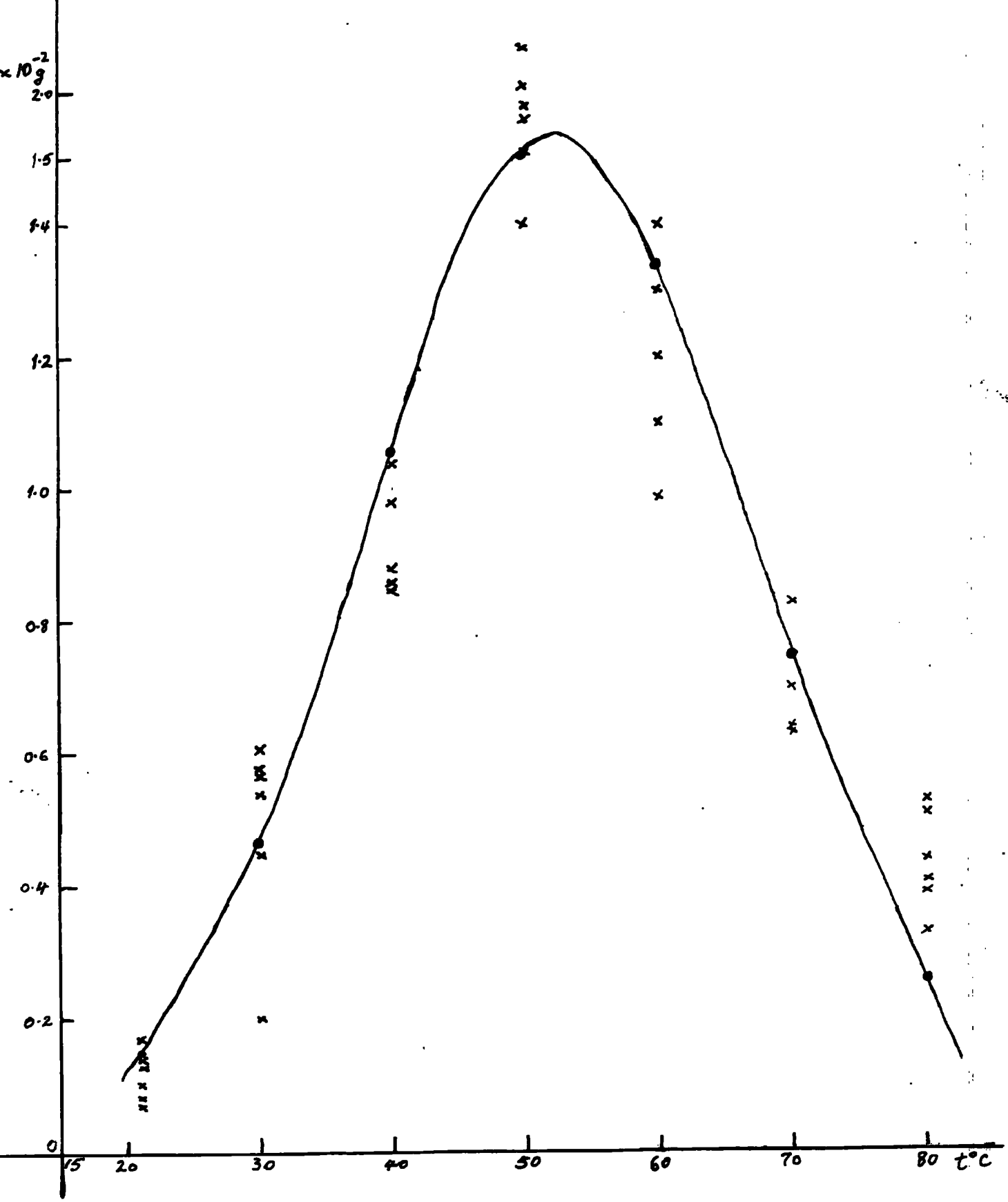

Fig.5.2. Cavitation erosion as a function of temperature for lead in water.

5.2 CONCLUSION.

The spread in the experimentally observed values in Figs. 5.1 and 5.2 are due to the length of time of operation (Erosion Method), the variations in the input voltage to the generator (Ch. 4); the random nature of cavitation and errors in the spectrophotometric spectrum plots (Chemical Method).

Sonochemical effects are aspects of cavitation relating to the gas-phase of the bubble and they depend on the gas-phase pressure effects. However, high vapour pressures inhibit cavitation phenomena and it is therefore not surprising that the intensity of cavitation, determined by the chlorine liberation method, should decrease as the temperature and hence the vapour pressure is increased. On the other hand, erosion effects are primary effects of cavitation occuring in the liquid-phase and they depend on the liquid phase pressure. The increase in cavitation erosion with rising temperature can be explained by the increase in the number of cavitation nuclei. By Eyring's theory of viscosity, plasticity and diffusion,(Ch. 2), molecules jump into existing holes in a liquid when they attain enough heat energy to surmount an activation potential barrier. With rising temperature, the probability of such jumps by molecules increases, the finite time for a small hole to grow in size to a hole large enough for complete rupture of the liquid decreases; and consequently, the number of erosion producing cavitation bubbles increases.

The presence of the maximum and its subsequent drop reveals a factor reducing damage, and this factor also increases with rising temperature. This is due to the damping of the shock waves (produced by the collapse of the cavities) by the inter-cavity pressure which increases with a rise in temperature and to a lesser extent to the decrease of the surface tension. The increase in

intercavity pressure with rise in temperature is the result of liquid vapour pressure and the pressure of gas dissolved in the liquid and penetrating into the cavities by diffusion. Hence, with rising temperature cavitation erosion will increase, due to the increase in the number of cavitation nuclei and the decrease in the strength of the liquid to withstand cavitation inception, to a maximum, after which the cushioning effects on shock waves takes over with a subsequent decrease in erosion.

In general, the results are in agreement with those of Weissler and Rosenberg and they suggest that the variations of the relative intensity of cavitation, measured by the chlorine liberation and erosion methods, are independent of the prevailing conditions - frequency of transducers, power input to the transducer, height of test samples over the transducer face, etc. Although mathematical expressions have been obtained for these two effects of cavitation (Eqns. 5.2 and 5.3); it must be remembered that due to evaporation effects, the accurate nature of Eq. 5.2 is unknown and hence Weissler's third proposition (the ratio a_i/b_i) can not be investigated. In the expressions

$$\sum_i a_i n_i \quad , \qquad \sum_i b_i n_i$$

Weissler described

(i) each i as the characteristic class of cavitation events (gassy or vaporous, steady-state or transient);

(ii) each n as the number of events of this class per second, per unit volume, under the specified set of conditions;

(iii) each a as a coefficient which expresses the relative cleaning effectiveness for this class of cavitation; and

(iv) each b as a coefficient of the relative sonochemical effectiveness for each class of cavitation.

It can be observed that although $\underline{i}$ and $\underline{n}$ may not be related, they both depend on the same factors as temperature, frequency, dissolved gas content, treatment time etc. Other factors that determine $\underline{i}$ include the latent heat of evaporation of the liquid, which, not only determines the ease of formation of vaporous bubbles but also influences the behaviour of bubbles at temperatures much less than or near the boiling point of the liquid; and also the power input to the transducer which determines the formation of steady-state or transient cavities. Furthermore, although chlorine liberation and erosion take place under cavitating conditions, the exact features of cavitation - noise, shock waves, sonoluminescence, etc. - responsible for chlorine liberation are not known; nor are the dependences of these features on the characteristic class of cavitation events, ($\underline{i}$), known. These factors suggest a totally new expression for each $\underline{i}$ and from the practical point of view, the determination of the ratio $^{a}i/b_{i}$ even at fixed temperature, frequency and treatment time is not simple.

Conditions governing the experimental set-up described above (Chs. 3 and 4) are similar to those that pertain in industrial cleaning; but no one of the two methods employed can be easily relied on as a means of determining cavitation intensity. The erosion method offers a good quantitative and qualitative measure in so much as it obtains in the liquid phase of cavitation but the preparation of test samples is a tedious process and the entire procedure is time consuming. Furthermore, there is no standard of finish of samples except that they must be of uniform finish. In the chlorine liberation method, the evaporation of carbon tetrachloride is a setback. Again, this reaction takes place in the gas phase of cavitation which may not have similar conditions as the liquid phase in which ultrasonic cleaning is

achieved. The erosion method suggests that ultrasonic cleaning is more efficient at about 50°C while the chlorine liberation method suggests a high efficiency at room temperature. It is necessary to conduct some experimental work with a view of determining the exact feature or features of cavitation responsible for chlorine liberation.

5.3 SUGGESTIONS.

An important factor that is more or less responsible for cavitation in the presence of an acoustic field is cavitation nuclei. The most reliable accessment of cavitation would be the counting of the cavitation nuclei in a liquid. The number of nuclei is bound to vary in different liquids and under different conditions; and consequently, the number of cavitation bubbles will vary. In most effects of cavitation, the important feature is the collapse of the bubbles and since each collapse is accompanied by the radiation of shock waves, the piezoelectric crystalline probe provides a means of detection of bubble collapses per unit volume, per second, under a specified set of conditions.

Under ultrasonic cleaning conditions, standing waves will be set up in the bath and this defines the best position for the crystals since at the nodal points, the acoustic pressure is zero. This means that the pressure on the crystal which will cause a difference of potential on the two parallel surfaces, will be due to the shock waves. The resulting potential difference may be low and by amplification, and feeding through a quenching unit to a scaling unit, the number of collapses can be obtained. If E_m is the amount of mechanical energy contained in the shock waves per unit volume, then the number of bubble collapses per unit volume, N, is proportional to E_m i.e.

$$N \propto E_m .$$

Similarly,

$$N \propto E_K$$

where E_K is the amount of acoustic energy used per unit volume in the formation of cavitation bubbles, and

$$E_{m/E_K} = \psi$$

will give the potential erosion efficiency of the cavitation process. The erosion efficiency η_{era}, of the acoustic field is

$$\eta_{era} = E_{m/E}$$

where E is the amount of acoustic energy introduced by the sound wave into a given volume.

Furthermore, it can be seen that

$$E_K = \sum_i E_i$$

where each $\underline{E}$ is the amount of energy used per unit volume for each cavitation process $\underline{i}$ (sonoluminescence, erosion, noise, etc). By the measurement of these other processes - noise [2.9], sonoluminescence [5.2], etc. - an accurate nature of E_K can be obtained and hence ψ. The piezoelectric probe will have the advantage of quick tests and can be applied with suitable crystalline materials for the determination of the variation of the relative intensity of cavitation with temperature. Furthermore, the intensity of the shock waves and hence the magnitude of the resulting potential difference on the faces of the crystal may yield some information as to the nature of the bubbles i.e. gassy or vaporous, steady-state or transient. This may yield values of $\underline{n}$ and $\underline{i}$ for a known treatment period and hence the ratio a_i/b_i can be calculated if the factors of cavitation responsible for chlorine liberation are investigated.

TABLE 5.1.

TEMPERATURE (^{o}C)	OPTICAL DENSITY (D_{436})
21	1.8329 ± 0.0659
28	1.3458 ± 0.0204
36	1.1313 ± 0.0172
45	0.8105 ± 0.0320
55	0.4771 ± 0.0183
65	0.3150 ± 0.0095
75	0.1495 ± 0.0141

TABLE 5.2.

TEMPERATURE (^{o}C)	LOSS IN WEIGHT (GMS).
21	0.0454 ± 0.0043
30	0.1955 ± 0.0172
40	0.3723 ± 0.0085
50	0.7490 ± 0.0548
60	0.4802 ± 0.0161
70	0.2707 ± 0.0085
80	0.1738 ± 0.0079

APPENDIX.

The computer analysis of the results was by method of least squares. First the computer obtained the plots of the best fitting curves, for each set of experimental results, in the form of the polynomial

$$y = a_o + a_1x + a_2x^2 + a_3x^3 + a_4x^4 \qquad \text{(i)}$$

From these curves, the form of the exponential equations were determined and the results fed into the computer for the co-efficients of the best fitting curves. For the erosion method, the equation used is in the form of a Gaussian

$$\Delta m = a. \exp \frac{-(T - c)^2}{b^2} . \qquad \text{(ii)}$$

From the shape of polynomial, (i), c was given values from 48 to 60; and the R.M.S. of deviations were 3.7×10^{-3} at c = 48 decreasing to 2.588×10^{-3} at c = 52, 2.601×10^{-3} at c = 53 and increasing to 4.147×10^{-3} at c = 60. There is not much difference between the R.M.S. of deviations at c = 52 and c = 53; and the value c = 52.5 was used. This gave an R.M.S. of deviations of 2.580×10^{-3}. Hence the value c = 52.5 in the expression for the variation of the relative intensity of cavitation with temperature by the erosion method.

REFERENCES.

1.1 Blitz, J., Fundamentals of Ultrasonics, Butterworths, London, 1963.

1.2 Vigoureux, P., Ultrasonics, Chapman & Hall, London, 1950.

1.3 Carlin, B., Ultrasonics, McGraw-Hill Book Co. Inc., New York, 1960.

1.4 Brown, B. and Goodman, High Intensity Ultrasonics: Applications, Iliffe Book Co. London. 1965.

1.5 Allen, C.H. and Rudmick, I., J. Acoust. Soc. Am., 19, 857, 1947.

1.6 Curie, J. and P., Comptes Rendus, 93, 1137, 1881.

1.7 Mason, W.P., Piezoelectric Crystals and Their Applications to Ultrasonics, B. Van Nostrand, N.Y. 1950.

1.8 Lippmann, G., Ann. Physique et Chimie, 24, 145, 1881.

1.9 Firestone, F.A., J. Acoust. Soc. Am., 17, 287, 1945.

1.10 Richards, W.T., Rev. Mod. Phys., 11, 36, 1939.

1.11 Lehmann, J.F. J. Acoust. Soc. Am., 25, 17, 1953.

1.12 Hueter, T.F. and Bolt, R.H., - ibid - 23, 60, 1951.

1.13 Brown, B., Industrial Electronics, pps. 44, 69, 113, 191, 1964.

1.14 Crawford, A.E., Butterworths Scientific Pub., Lond., 1955.

1.15 Jones, J.B. and Powers, J.J., Welding J., 35, 761, 1956.

2.1 Horton, J.P., J. Acoust. Soc. Am., 25, 480, 1953.

2.2 Willard, G.W., - ibid - 25, 669, 1953.

2.3 Fisher, J.C., J. Appl. Phys., 19, 1062, 1948.

2.4 Messino, D., Sette, D. and Wanderluigh, F., Proc. 4th Int. Cong. Acoust., J. 34, 1962.

2.5 Sette, D., Proc. 3rd Int. Cong. Acoust., 330, 1959.

2.6 Pease, D.C. and Blinks, L.R., J. Phys. Cell. Chem., 51, 556, 1947.

2.7 Plesset, M.S., Cavitation in Real Liquids, Elsevier Pub. Co. Ltd., 1964.

2.8 Macleay, R. and Holroyd, L., J. Appl. Phys., 32, 449, 1961.

2.9 Boucher, R.M.G., Measurement of Ultrasonic Cavitation, Private Comm., 1965.

2.10 Slater, J.C., Physics Today, 2, 6, 1949.

2.11 Finch, R.D., Ultrasonics, 1, 87, 1963.

2.12 Marinesco, N. and Trillab, J.J., Compt. Rend., 196, 858, 1933.

2.13 Ernst, P.J., J. Acoust. Soc. Am., 23, 80, 1951.

2.14 Lord Rayleigh, Phil. Mag., 34, 94, 1917.

2.15 Beeching, R., Trans. Inst. Eng. Shipb. Scat., 85, 273, 1942.

2.16 Silver, R.S., Engineering, 154, 501, 1942.

2.17 Knapp, R.R. and Hollander, A., Trans. Am. Soc. Mech. Eng., 70, 419, 1948.

2.18 Plesset, M.S., J. Appl. Mech., 16, 277, 1949.

2.19 Noltingk, B.E. and Neppiras, E.A., Proc. Phys. Soc., 63B, 674, 1950.

2.20 Noltingk, B.E. and Neppiras, E.A., Proc. Phys. Soc., 64B, 1032, 1951.

2.21 Sirotyuk, M.G., Soviet Phy. Acoust. 7, 4, 499, 1961.

2.22 Khoroshev, G.A. -ibid- 9, 3, 275, 1964.

2.23 Eller, A. and Flynn, H.G., J. Acoust. Soc. Am., 37, 493, 1965.

2.24 Weissler, A., J. Chem. Educ., 25, 28, 1948.

2.25 Brown, B. and Grange, A., Brit. Comm. Electronics, 1961.

2.26 Griffing, V., J. Chem. Phys. 18, 997, 1950.

2.27 Eisenberg, P., Technical Report 233 - 1, U.S. Naval Res. 1963.

2.28 Plesset, M.S. and Ellis, A.T. Trans. A.S.ME. 7, 1055, 1955.

2.29 Bebchuk, A.S. Sov. Phys. Acoust., 3, No. 1, 1957 and No. 4, 1957.

2.30 Wilson, R.W. and Graham, R., Conference On Lubrication and Wear, Inst. of Mech. Eng., Lond., 1957.

2.31 Rosenberg, L.D. and Siratyuk, M.G., Sov. Phys. Acoust., 6, 477, 1961.

2.32 Sirotyuk, M.G., Sov. Phys. Acoustics, 7, 405, 1962.

3.1 Joule, J.P., Phil Mag., 30, 46, 1847.

3.2 Pierce, G.W., Proc. Am. Acad., 63, 1. 1928.

3.3 Wise, B.A., "Design of Nickel Magnetostrictive Transducers" Int. Nickel Co. Ltd., 1957.

3.4 Butterworth, S. and Smith, F.D., Proc. Phys. Lond., 59, 19, 1947.

3.5 Camp, L., J. Acoust. Soc. Am., 20, 616, 1948.

3.6 Leslie, F.M. - ibid - 22, 418, 1950.

3.7 Bozorth, R.M., Ferromagnetism, Van Nostrand Co. Ltd., 1951.

3.8 "Annealing Nickel, Monel, Inconel", Inco.Tech. Bull., T20.

3.9 Richardson, E.G., Tech. Aspects of Sound., Elsevier, 1957.

3.10 Gollmick, H.J., Metal Finishing Jour., May-June, 1962.

4.1 Bebchuk, A.S., Akust. Zhur., 3, 90, 1957.

4.2 Bennett, G., J. Acoust. Soc. Am., 24, 470, 1952.

4.3 Neppiras, E.A. Ultrasonics, 3, 9, 1965.

4.4 Weissler, A. IRE. Int. Convention Record, 1962.

4.5 Rosenberg, L.D., Ultrasonic News, 17, Winter, 1960.

4.6 Shih-Ping Liu, J. Acoust. Soc. Am., 38, 817, 1967.

5.1 Neppiras, E.A. and Parrott, J., 5th Int. Cong. Acoust., D.51, 1965.